

## THE ROMAN VILLA OF POSITANO (CAMPANIA REGION, SOUTHERN ITALY): PLASTERS, TILES AND GEOARCHAEOLOGICAL RECONSTRUCTION

Sossio Fabio GRAZIANO<sup>1</sup>, Concetta RISPOLI<sup>2</sup>, Vincenza GUARINO<sup>2</sup>, Giuseppina BALASSONE<sup>2,3,4\*</sup>, Giovanni DI MAIO<sup>5</sup>, Lucia PAPPALARDO<sup>6</sup>, Piergiulio CAPPELLETTI<sup>2,3,7</sup>, Giulio DAMATO<sup>8</sup>, Alberto DE BONIS<sup>2,3</sup>, Claudia DI BENEDETTO<sup>2</sup>, Loredana D'ORAZIO<sup>4</sup>, Vincenzo MORRA<sup>2,3,9</sup>

<sup>1</sup> Dipartimento di Farmacia, Università di Napoli Federico II, Via Domenico Montesano, 49, Napoli, Italy 80131

<sup>2</sup> Dipartimento di Scienze della Terra, dell'Ambiente e delle Risorse, Università di Napoli Federico II, Via Cintia, 26 - Napoli, Italy 80126

<sup>3</sup> Center for Research on Archaeometry and Conservation Science, CRACS, Università di Napoli Federico II, Italy, Università del Sannio, Italy

<sup>4</sup> Istituto per i Polimeri Compositi e Biomateriali IPCB, CNR, Via Campi Flegrei, 34, 80078 Pozzuoli, Naples, Italy

<sup>5</sup> GEOMED Geoarcheologia & Ambiente, Via L. Sicignano 40, Scafati, Salerno, Italy 84018

<sup>6</sup> Istituto Nazionale di Geofisica e Vulcanologia, Osservatorio Vesuviano, Via Diocleziano 328, Napoli, Italy 80124

<sup>7</sup> Centro Museale "Centro Musei delle Scienze Naturali e Fisiche", Università Federico II, Via Mezzocannone, 8, Napoli, Italy 80134

<sup>8</sup> Freelancer, Via Adolfo Albertazzi, 92, Roma, Italy 00137

<sup>9</sup> Centro Interdipartimentale di Studi per la Magna Grecia, CISMIG, Università di Napoli Federico II, Italy

### Abstract

A Roman luxury villa (1<sup>st</sup> century BC) was discovered in the town of Positano, in the Sorrento peninsula (Campania region, southern Italy). Despite being more than 20 km away from Vesuvius, the villa was buried under almost overall 20 meters (total thickness) of pyroclastic materials of the Plinian eruption of 79 AD, which destroyed Pompeii and Herculaneum towns. The exceptional level of conservation of this residential complex is due to the peculiar burial process, which determined the excellent state of preservation of both the fresco decorations (Fourth Style) and all other artefacts (masonries, plasters, tiles, furnishing remains, wooden elements, kitchenware, glazed oil lamps, bronze vessels and other metallic findings, etc.). This study presents the results of a multi-analytical archaeometric analysis of plasters, fresco pigments and roof tiles, aimed at identifying their mineralogical and petrographic nature and the provenance of raw materials. Constraints to the geoarchaeological landscape of the Positano area are also given. The analyzed plasters are mainly lime-based, usually with the addition of an aggregate. The anchoring layer is made by a volcanic component, characterized by clinopyroxene, alkali feldspar, garnet, amphibole, biotite and leucite crystals, together with a sedimentary component represented by carbonatic fragments, also with traces of microfossils. The features of plasters confirm the high degree of technological standardization of plasters in classical Roman age. Mineral pigments recognized by preliminary XRD are mainly iron-based for the ochers-red-crimson colors and copper-based for green-blues colors. In the roof tiles two kind of tempers are identified. In three samples a volcanic temper was identified, and represented by clinopyroxene, feldspar, garnet and leucite, whereas the temper of a fourth sample contained pumices with minor amounts of alkali feldspar, clinopyroxene and biotite. The raw materials are of local provenance (Somma-Vesuvius, Phlegraean Fields, Apennine limestones), and the microstructure of the materials are comparable with similar artefacts from Pompeii, Herculaneum and other Roman sites in Campania region. On the basis of geoarchaeological investigations, here reported, it is reasonable to think that there are other unearthed archaeological areas in Positano that will require further study to be properly known.

**Keywords:** Positano; Roman villa; southern Italy; Vesuvius; Pompeii eruption; Plasters s.s.; Arriccio; Pigments; Tiles; Geomaterials; Geoarchaeological landscape

\* Corresponding author: balasson@unina.it

## Introduction

The Campania Region, in the south of Italy, has plenty of worldwide renowned archaeological sites, such as those occurring in the areas nearby the Bay of Naples, from Pompeii, Herculaneum, Oplontis, Paestum and Velia in the central-southern areas, to Baia and Cuma in the northern part, among many others (Fig. 1a). Beyond these sites, other minor but absolutely not less important archaeological remains (villas, amphitheatres, cisterns, thermae, necropolis, etc.) are widespread in the whole region, and were object of many archaeometric investigations [1,2,11,3–10]. The luxury Roman villas, especially those present in the Bay of Naples, are famous and some well-documented, whereas the southern side of the Sorrento peninsula (named from the town of Sorrento; Fig. 1a) overlooking the Bay of Salerno, now commonly known as the Amalfi Coast, was also a venue for maritime Patrician villas, built by early Julio-Claudian times, and possibly earlier [12].

Along the Amalfi coast of the Sorrento peninsula, a Roman villa (1<sup>st</sup> century BC) was discovered in the town of Positano, under the main church of S. Maria Assunta (Figs. 1b,c). Despite the distance from Vesuvius (more than 20 km away) and the low position, protected to the north by the mountains, the villa was initially buried by the products of 79 AD Vesuvius eruption, under almost 2 meters of fallout material and overall 20 meters of pyroclastic materials [12]. According to [13], the emperor Claudius may have built a villa on the south coast of the Sorrento peninsula, whereas [14] affirmed the name Positano may have a toponomastic derivation from *Posidetanum (praedium)* (“property of Posides”), from the name of the freedman Posides, owner of the villa [12].

The presence of ancient remains under the medieval church of S. Maria Assunta had been already known several centuries ago; extensive excavations had been carried out in the late 1600s, to recover colored marble and architectural pieces, and in 1758 Karl Weber, the engineer of the royal Bourbon administration of Naples and the director of excavations at Pompeii, Herculaneum, and Stabia, started excavating beside the church, after the recovery of ancient remains during works to consolidate the bell tower [12] (and references therein). In the 1920s new parts of the villa were discovered at the back of a butcher’s shop; some digging revealed the corner of a peristyle already identified by Weber in 1758, with several stuccoed columns [15,16]. A devastating flood in 1954 brought to light additional structures belonging to the villa, which Amedeo Maiuri, the director of excavations at Pompeii at the time, rightly identified as part of a villa buried by the 79 AD event [17].

Starting in 1999, the Soprintendenza of Salerno conducted a series of geo-archaeological investigations in order to reconstruct the extent of the archaeological complex buried under the church of S. Maria Assunta, bell tower, and surrounding gardens. Then, in 2003 stratigraphic investigations in the crypt of the Church of S. Maria Assunta were carried out. This work was constrained by the small size of the workable area and the need to consolidate the ancient structures and wall paintings while the excavations proceeded. Two campaigns of excavations, structural reinforcements and restoration (2004-2006 and 2015-2016) have brought to light a portion of the Roman villa, unearthing the entire north and the east walls of the room, down to its simple white mosaic floor framed by bands of black tesserae. Large fragments of a third wall on the west side have been found in situ, while the south side may have opened to a view of the sea or toward a peristyle; a stuccoed column collapsed into the room suggests a peristyle portico or a terrace with a colonnade [12].

The public opening of the whole structure, now called MAR Museo Archeologico Romano of Positano (<https://marpositano.it>), took place in the summer of 2018; the public access starts from the medieval hypogeum and reaches the villa with a system of suspended walkways (catwalks and stairs).

The Positano villa, as the other rich maritime villas of the Amalfi Coast, was overcome first by the material from the fallout of the Vesuvian 79 AD Plinian eruption, then immediately

afterwards by the violence of the flow-slides (Fig. 1b). The exceptional level of conservation of this residential complex is the direct result of this particular burial process, which determined the excellent state of preservation of both the wall decorations and all the other artifacts. However, these remains have also provided important information for the geological reconstruction of the ancient landscape [19]

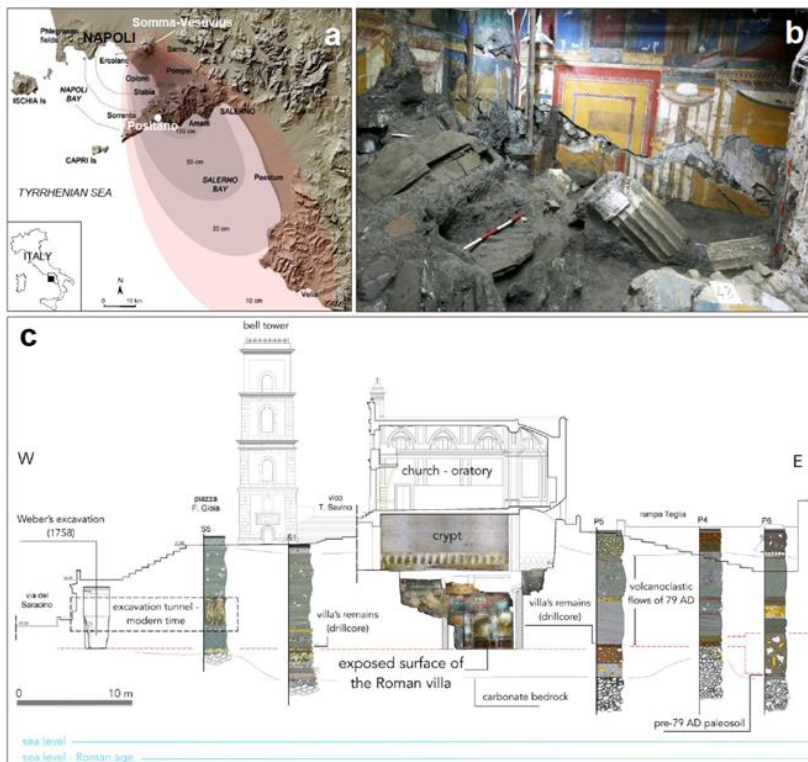


**Fig. 1.** (a) The Campania region (southern Italy) and location of Positano, with isopach map of the Vesuvius Pompeii (AD 79) pyroclastic fall (red shaded areas) and flows (red lines) (modified from [18]). (b) The triclinium of the Roman villa, in an advanced phase of the last excavation works (2015-2016, see text), with the eastern wall showing a clear displacement (ca. 40 cm) due to the southward volcaniclastic flow of the 79 AD eruption; a stucco's column, likely related to the southern peristyle located on the south side of the dining room (open toward the sea), is in the foreground [18] (c) W-E cross-section of the investigated area of the S. Maria Assunta church, the underlying medieval hypogeum and the Roman villa, where P4, P5, P6, S1 and S5 are the geoarchaeological drillcores (modified from [19]).

This study aims to (i) characterize the mortars/plasters, fresco pigments and roof tiles used in the construction of Roman villa of Positano, in order to improve the knowledge about Roman construction material manufacturing by means of a detailed microstructural and compositional examination of the geomaterials (i.e. the aggregates for mortars, etc.; [2,20]) as well as to gather information for planning restoration and conservation activities, (ii) identify the provenance of raw materials, and (iii) define the geoarchaeological landscape of the Positano area.

**Geological and archaeological outline**

The town of Positano is located in the Amalfi Coast in the southern sector of the Sorrento Peninsula (Figs. 1a and 2), formed by the Lattari Ridge which belongs to the westernmost sector of the southern Apennines [21]. This area mainly consists of Mesozoic carbonaceous successions (Jurassic and Cretaceous), along with lithologies of more recent syn-

orogenic deposits, such as the Reconnome calcarenites (lower Miocene) and sandstones formation, part of the Southern Apennine domain [22,23].

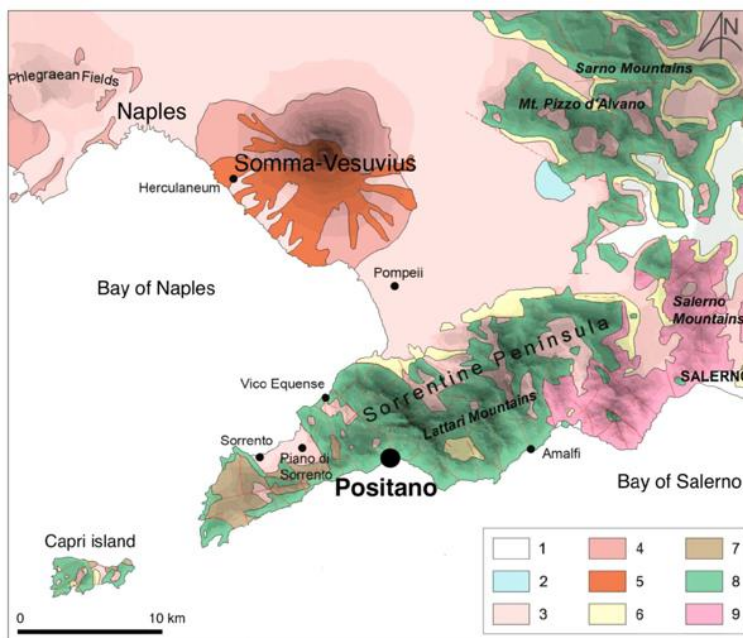


**Fig. 2.** Geological map of the area surrounding Positano, in the Sorrentine Peninsula, up to Somma-Vesuvius volcano and the Phlegraean Fields areas (1 = alluvial deposits; 2 = travertine; 3 = incoherent ash-fall deposits; 4 = mainly coherent ash-flow deposits; 5 = lavas; 6 = detrital deposits; 7 = Miocene flysch; 8 = Middle Jurassic-Upper Cretaceous limestones; 9 = Lower Triassic-Middle Jurassic dolomites and calcareous limestones; solid and dotted red lines are outcropping and buried faults). Modified from Apuzzo et al. (2013).

The most recent formations are alluvial deposits, also formed by, more or less reworked, volcanic products of Somma-Vesuvius complex mainly deriving from products of the 79 AD eruption [24,25] as well as from deposits related to Phlegraean Fields activity (Campanian Ignimbrite, 39 ka; [26], and references therein). Despite the morphological protection by the steep Lattari Mountains and the distance from the Vesuvius volcano, the 79 AD eruption that destroyed Pompeii had also affected the Amalfi Coast. The eruptive column of gas and ash ejected up to 30 km into the atmosphere where prevailing winds then pushed it southward (Fig. 1a). About 2 meters of pumice and ash fell in the Porto gulley - the basin of the Positano Marina - and on a large part of the Gulf of Salerno [27]. The resulting volcanoclastic incoherent and unstable materials could not remain balanced on the steep and rugged limestone slopes of the Lattari Mountains, hence pyroclastic material entered the buildings through doors and windows and, as it accumulated on the roofs, it caused them to collapse. Almost simultaneously, the large quantities of pyroclastic material that fell on the steep slopes of the Lattari Ridge slid downhill, generating lahars or volcanoclastic flows moving at high speed, with devastating consequences for whatever they hit in their path. The accumulations completely destroyed the Positano villa: the ground level rose about 20 m in some places and the shoreline advanced, as attested by the identification of a fan-shaped accumulation subsequently dismantled by marine erosion [12]. A particular feature of the lithologies occurring in this area is the high reactivity of the pyroclastic materials, that quickly solidified into a tuffaceous rock, so hard that its modern excavations must use jackhammers. This material is locally known as “*Durece*” [2] (and references therein) and has been widely used in building construction [27]. The geoarchaeological investigations

indicate that a thin layer of ash first fell on the villa, followed by thick pumice fall deposit that buried it about 2 meters deep (Fig. 1c). The sloping roof of the *triclinium* directed much of the pumice toward the gardens and the external spaces of the villa. Part of the wooden structures composing the roof and attic collapsed, falling in a vertical position on the furnishings inside the space. At the same time, other lobes of the flow reached the peristyle, flowed back uphill into the *triclinium* up against its northern wall, dragging the columns of the portico and all the artifacts. Already partially filled, the walls of the *triclinium* began to collapse under the increasing weight of the volcanic mud flowing downhill from higher elevations. The northern and eastern walls remained almost intact (Figs. 3a,b), but were broken off at a height of 1.5 meters from the pavement, whereas the western wall was smashed into pieces and only few parts were found in-situ (Figs. 3c). The upper part of the broken wall(s) moved about 40 cm downhill but did not fall over, indicating that the southern lobe of the flow had already rapidly filled the *triclinium* (Figs. 1b and 3b) [19,27].



**Fig. 3.** (a) The north wall of the triclinium in the Positano villa; an ash cast of a door is visible at the left corner, leading to other not yet explored frescoed room (photogrammetry reconstruction, photos by G. Di Maio, Geomed archives). (b) The east wall of the triclinium room (photogrammetry reconstruction, photos by G. Di Maio, Geomed archives). (c) The in-situ part of the west wall (Geomed archives). (d) Detail of the collapsed walls, with yellow tuff cubilia of opus reticulatum and tiles of the pitched roof (excavation phase on 19th 2015; photogrammetry reconstruction, photos by G. Di Maio, Geomed archives). Bar length for images (a) and (b) is 2 m; the images width is ca. 60 cm in (c) and 5 m in (d).

A great variety of objects - furnishing remains, wooden elements, kitchenware, glazed oil lamps, bronze vessels and other metallic findings, tiles, etc. - are found in the Positano's villa and are currently under investigations [28]. As concerns the wall paintings, corresponding to the mature Fourth Style (Figs. 3a-c), their high artistic quality draw peculiar interest, indicating the villa's opulence as well as a very refined taste and high standards of the artists; they likely coming from Rome and probably in relation to the imperial court artists in service at Capri island. The decorative scheme is unusual for private houses, with abundant use of white stucco molded in relief in the upper part of the wall decoration for figures of cupids and fantastic animals. The colors of wall decorations are rich ranging from azure-blue to green, from red to yellow; in particular, the blue colors, very expensive pigments and largely used for the backgrounds of the paintings, reflect the wealth of the owner of the villa. The artists at Positano

intended to achieve maximum scenographic effect and the originality of frescoes is evident when compared to other examples from the Vesuvian area [12].

At the moment of its destruction, the villa was probably undergoing renovations. A large iron saw found in the *triclinium* attests work-in-progress, and a test trench opened to the southeast of the church has revealed *opus reticulatum* walls (Fig. 3d) and a large pile of the typical diamond-shaped bricks composed of Neapolitan yellow tuff (*cubilia*) freshly roughed out, to be used in *opus reticulatum* wall facings. Tufa chips and unfinished elements indicate that the *cubilia* were being shaped in situ [12].

#### ***Natural and artificial geomaterials in the Campania region***

Since ancient times in the Campania region there was a large use of local geomaterials for constructions, masonry, artistic works, etc. A large variety of stones were used, both of volcanic and sedimentary origin, such as pyroclastic rocks (tuffs, ignimbrites), lavas, limestones, travertines, and so on [29,30].

As concerns the volcanic lithotypes, the Campanian Ignimbrite deposit (CI) and Neapolitan Yellow Tuff (NYT) are the most important geomaterials used in Campania region both derived from Phlegraean Fields volcanic activity [29,31] (Fig. 2). The CI (~40 ka) deposit had an original areal distribution of at least 1500 km<sup>2</sup> and extends from Naples up to the province of Caserta, more than 40 km north of Naples [32–35]. It is buried underneath more recent sediments or other volcanic products, as in the Volturno Plain, in the Phlegraean Fields and in the Somma-Vesuvius areas; sometimes it has been partly or totally eroded. The original extent of the ignimbrite was almost as large than now, creating a continuously covered area that extended from Naples to Lazio region, from the Apennine massifs and to the Tyrrhenian sea. The typical ignimbrite grey facies consist of pumice and lithic fragments of variable size placed in a matrix made of ash. Pumice generally contains sanidine, minor biotite and clinopyroxene phenocrysts that are placed in the matrix; its composition is trachytic [36]. *Piperno* is another important geomaterial in the Campania region, and corresponding to one of the six stratigraphic units of the *Breccia Museo*, a volcanic formation related with the Campanian Ignimbrite-forming eruption; along with the NYT is the main lithotype of Phlegraean Fields activity [32,34].

The NYT (15 ka) is the second largest pyroclastic deposit of the Campanian volcanic area after the CI [37]. The eruption was first a central-vent episode then turned into a multiple-vent episode, with phreatomagmatic and magmatic phase following the caldera collapse. The NYT owes its name from the yellow color due to zeolitization only in areas close to the vent [31]. The composition varies from latite to alkali trachyte, and rocks are mainly aphyric or sub-aphyric. The phenocrysts represent less than 3% of the total volume and are mostly sanidine, plagioclase, biotite, magnetite and apatite.

Together with pyroclastic deposits, lavas from the Phlegraean Fields been also employed in building activity of Campania region from ancient times. In the Phlegraean Fields, after each caldera formation, the activity was mostly explosive; limited trachitic lavas are present in some sites, i.e. Astroni, Monte Spina, Cuma, Punta Marmolite and Monte Olibano. This last occurrence is the most important lava outcrop and interested by an intensive extractive activity. Lava from Phlegraean Fields district shows a porphyritic fabric, with phenocrysts mostly represented by sanidine and subordinated clinopyroxene. Microcrystals of magnetite and plagioclase, olivine, apatite and biotite can also occur.

Even though the Somma-Vesuvius volcanism started about 400 ka BP (<sup>40</sup>Ar/<sup>39</sup>Ar ages, Trecase core), the present volcanic complex was formed just after the emplacement of the CI, <40 ka [38], with the most recent lavas erupted in 1944 AD.. Its volcanic activity ranges from effusive to Plinian; it is estimated that with every Plinian event between 5 and 10 km<sup>3</sup> of pyroclastic materials were produced. Somma-Vesuvius products display, with very few exceptions, potassic to ultrapotassic affinity, exhibiting a wide variability from nearly silica-saturated (normative nepheline <5%) to silica-undersaturated (leucite-normative). During the

last ~22 ka, Somma-Vesuvius activity was characterized by alternation of explosive eruptions, whose products show juvenile fraction as pumice and scoria fragments, and effusive episodes, with emplacement of lava flows [25]. The composition of Somma-Vesuvius products is mainly high to ultra-potassic ( $K_2O = 2.3\text{--}9.6$  wt%;  $SiO_2 = 47\text{--}59$  wt%). The potassium content and silica-undersaturation increase with time, together with the ratio of discriminative trace elements. The degree of silica undersaturation and potassium enrichment has been used to distinguish different magmatic series; products older than 8.9 ka consists of porphyritic slightly silica-undersaturated basic potassic rocks, whose compositions straddle the boundary between shoshonite-latitude and tephrite-phonolite fields on TAS diagram. Products ranging from ~8.9 ka to 2.7 ka are characterized by a mildly silica-undersaturated series (phonotephrites, tephriphonolites and phonolites richer in alkalis compared with the previous group). Products younger than 79 AD are composed of strongly silica-undersaturated leucite tephrites, leucitites, phonotephrites, tephriphonolites, foidites and phonolites with a distinctive porphyritic texture [25] (and references therein).

Sedimentary rocks of the Campania region used as building stone materials have been important as the volcanic rocks since Greek and Roman ages. A large variety of sedimentary lithotypes have been utilized for every type of constructions and artifacts, from historical times up today. They range from Mesozoic to Cenozoic in age, and include many renowned industrial stones in Italy, such as the *Mondragone* and *Vitulano-Cautano* "marbles", the *Irpina* "breccia", the "stones" of *Bellona*, *Cusano*, *Padula*, *Roccadaspide*, *Bisaccia*, *Fontanarosa*, as well as travertines and alabasters. However, an extended treatment of the sedimentary building stone from Campanian outcrops can be found in [29].

In the Roman imperial period, both natural (tuffs, ignimbrites, lavas, sedimentary rocks) and artificial (mortars, plasters, brick, pigments, etc.) geomaterials were used in Campania region, often as result of a high level of expertise. Since the late republican period of Roman age, mortars have been used for various purposes like decoration of buildings walls, preparing frescos surfaces and decorations etc. The durability of Roman mortars is due to the excellent quality of raw materials, very high quality of technological processes and standardized methods of application and production.

Pliny the Elder described the use of lime, used by Romans many ways for the preparation process of various kinds of mortars. Cato's *De Agricola* (160 BC), Pliny's *Naturalis Historia* and Vitruvius Pollione's *De Architectura* (1<sup>st</sup> century BC) also mentioned this practice of Romans. Romans knew that some volcanic deposits, if mixed with lime, could have been used to create high quality mortars with higher mechanical and water resistance, i.e. the pozzolan. Vitruvius explained how the use of pozzolan triggered a revolutionary progress in construction activities, thanks to the mixture's capacity to harden also underwater. When volcanic materials were unavailable, Romans used artificial materials in fragments, i.e. crushed bricks and ceramic fragments [1], which have as the same properties as pozzolan. Vitruvius also described *cocciopesto*, a term which refers to a particular technique of building construction widely used by Roman architects for its considerable technical features as result of pozzolan component [1].

The pozzolan described by Vitruvius was produced starting from the NYT (see above), mainly coming from the upper part (grey facies) of the succession. Pozzolan, with its contents of silica and alumina, is capable of reaction with hydrated lime, allowing the formation of hydrate calcium silicates (C-S-H) in a relatively short time. The C-H-S materials are characteristically stable and insoluble. The typical production of lime includes heating of carbonaceous rocks (calcination) up to 850-900 °C, dissolving calcium carbonate ( $CaCO_3$ ) to create  $CO_2$  and CaO (quicklime). To be used as a binder, CaO reacts with water, giving  $Ca(OH)_2$  (slaked lime).

In ancient times, both river and beach sands were adopted in the aggregates, mixed with water and hydrated lime for air lime production. Afterwards, the discovery of volcanic sand,

instead of river or beach one, as aggregate component led the mortars to become hydraulic and useful also underwater [1].

## Experimental

### Materials

The last geoarchaeological campaign of the Positano villa's site and the surroundings, before the restoration and the public opening, was carried out during 2015-2016 by Geomed S.r.L.. A total number of 25 representative geomaterials (21 plasters and 4 roof tiles; Table 1) were collected for the present work during excavation campaign from the west wall of the *triclinium* (Fig. 4a), with the assistance of archaeologists of the former Soprintendenza per i Beni Archeologici della Campania.

**Table 1.** The studied samples: labels, typologies and description.

#	Sample ID	Geomaterial	Number of layers	Painting color
1	VP1	plaster ( <i>arriccio</i> )	1	
2	VP4	plaster (plaster s. s.)	1	
3	VP8a	plaster ( <i>arriccio</i> )	1	
4	VP8b	plaster ( <i>arriccio</i> )	1	
5	VP9	plaster ( <i>arriccio</i> , plaster s.s., mural painting)	3	ocher/brown
6	VP13a	plaster (plaster s.s., preparation layer, mural painting)	3	ocher
7	VP13b	plaster ( <i>arriccio</i> , plaster s.s., preparation layer, mural painting)	4	red
8	VP13c	plaster (plaster s.s., mural painting)	2	purple
9	VP13d	plaster (plaster s.s., mural painting)	2	crimson/blue
10	VP13e	plaster ( <i>arriccio</i> , mural painting)	2	green
11	VP13f	plaster (plaster s.s., mural painting)	2	blue
12	VP13g	plaster ( <i>arriccio</i> , plaster s.s., preparation layer, mural painting)	4	pink/orange
13	VP15a	plaster ( <i>arriccio</i> )	1	
14	VP15b	plaster ( <i>arriccio</i> )	1	
15	VP15c	plaster ( <i>arriccio</i> )	1	
16	VP16	plaster ( <i>arriccio</i> )	1	
17	VP17	plaster ( <i>arriccio</i> )	1	
18	VP18	plaster ( <i>arriccio</i> )	1	
19	VP19	plaster ( <i>arriccio</i> )	1	
20	VP20	plaster (plaster s.s., mural painting)	2	blue
21	VP21	plaster (plaster s. s.)	1	
22	VP12a	roof tile		
23	VP12b	roof tile		
24	VP12c	roof tile		
25	VP12d	roof tile		

### Methods

Fragments of collapsed masonries of this side of the *triclinium* were studied by means of the macro- and microstratigraphic description of binding materials suggested by the Ente Italiano di Normazione (UNI 11305: 2009 standard), using various combined techniques described below. Plasters were studied following definitions and layer classification as reported in literature [39,40], considering both macro-to-micro-textural and compositional characteristics (Fig. 4b and Table 1).

All the samples were studied in thin sections by means of Polarizing Optical Microscopy (POM) using transmitted light Laborlux 12 POL polarizing microscope equipped with a Carl Zeiss Axiocam 105 color (5 megapixel resolution) and Carl Zeiss ZEN digital imaging analysis software; observation helped to distinguish textures and petrographic characteristics of samples, such as crystals, groundmass, other inclusions, etc., described according to the [41].



**Fig. 4.** (a) Recomposition of fragments belonging to the west wall (photos by G. Di Maio, Geomed archives); image width ca. 2 m. The samples of this study come from this part of the triclinium; (b) sketch section of a typical Roman plaster, inferred from the Vitruvius' treatise, redrawn after [39].

As regards plasters, different layers were described following the [41] standard regulations which define: presence of aggregate, aggregates grain size, groundmass distribution, sorting, fitting, orientation, composition, morphology and clast aspect, kind of binding and its porosity.

Qualitative mineralogical analyses were performed by X-ray powder diffraction (XRPD) using an automatic diffractometer Panalytical X'pert PRO along with a Panalytical PW1730 with a MPD PW 3710 unit, both equipped with X'Pert data collector 2.1 software for data acquisition and X'Pert Highscore Plus 3.04 for pattern interpretation. Operation conditions were:  $\text{CuK}\alpha$  radiation, 40 kV, 40 mA,  $2\theta$  interval from  $4^\circ$  to  $50^\circ$ , step size =  $0.020^\circ$   $2\theta$  counting time 120 seconds per step.

Micro-textural observations and quantitative microanalyses were carried out by Scanning Electron Microscopy coupled with Energy Dispersive Spectroscopy (SEM-EDS), with a JEOL JSM-5310 (Jeol Ltd., Tokyo, Japan) instrument. An Oxford Instruments Microanalysis Unit (Oxford Instruments plc, Abingdon, Oxfordshire, UK) equipped with an INCA X-act detector (ETAS group, Stuttgart, Germany) was used. Measurements were performed with an INCA X-stream pulse processor (ETAS group, Stuttgart, Germany) using a 15kV primary beam voltage, 50–100  $\mu\text{A}$  filament current, variable spot size, from 30,000 to 200,000 $\times$  magnification, 20 mm WD and 50 s net acquisition real time. The INCA Energy software (ETAS group, Stuttgart, Germany) was employed, using the XPP matrix correction scheme and the Pulse Pile up correction. The quant optimization was carried out using cobalt (FWHM—full width at half maximum peak height of the strobed zero = 60–65 eV). The following standards from the Smithsonian Institute and MAC (Micro-Analysis Consultants Ltd. St Ives, UK) were used for calibration: diopside (Ca), fayalite (Fe), San Carlos olivine (Mg), anorthoclase (Na, Al, Si), rutile (Ti), serandite (Mn), microcline (K), apatite (P), fluorite (F), pyrite (S), sodium chloride (Cl), benitoite (Ba) and pure vanadium (V). The  $\text{K}\alpha$ ,  $\text{L}\alpha$ ,  $\text{L}\beta$ , or  $\text{M}\alpha$  lines were used for calibration, depending on the specific element. High-resolution imaging of surface morphology (backscattered images) was generated by secondary electrons using the same instrument.

Pumices and minerals have been analyzed by means of EDS in thin section (Energy Dispersion System, JEOL JSM-5310 electron microscope, equipped with an INCAx-Act detector), in order to evaluate the quantitative chemical composition (expressed as main element oxides in wt%).

Selected samples (plasters and tiles) were examined by X-ray computed microtomography ( $\mu\text{-CT}$ ), a totally non-destructive technique that generates digital 3D maps of the inner part of a solid sample (crystals size and orientation, pores, etc.) with a high spatial and density resolution (< 1 micron). Using a rendering software is possible to reconstruct the entire volume with the opportunity of virtually cutting the sample to observe the inner structure.

The  $\mu$ -CT instrument used for this work is a Carl Zeiss Xradia Versa-410 system, equipped with a polychromatic X-ray source (150 kV 10W microfocus), and a (2k x 2k pixel, noise suppressed charge-coupled) detector furnished of microscope objectives with magnifications ranging from 0.4X to 20X allowing spatial resolution up to 0.9 micron (Istituto Nazionale di Geofisica e Vulcanologia, Osservatorio Vesuviano).

A subset of samples was further examined by means of FTIR spectroscopy operating in transmission mode at room temperature. A Perkin-Elmer Spectrum 100 spectrophotometer was used. The instrumental parameters adopted were as follows: resolution  $4\text{ cm}^{-1}$  and spectral range  $4000\text{-}400\text{ cm}^{-1}$ . KBr classical pellet method was applied on powder samples.

## Results and discussion

### Plasters

Samples were studied dividing them into different layers accordingly to Roman plaster model [39]. On the basis of their macro-to-micro-textural and compositional characteristics, each layer was studied independently (Table 1, Fig. 4b).

For each layer typology of the studied samples (Fig. 5 and 6), macroscopic results can be summarized as follows:

- **arriccio** - generally used to cover the structure of the wall/ceiling of masonries and shows 2 to 8 cm in thickness. These samples have a brown-grey matrix with usually well sorted aggregates both of sedimentary and volcanic origin.
- **plaster s.s.** - it follows the *arriccio* and represents a finer layer, for this reason samples have a lighter color matrix (yellowish-white) with fine size aggregates both of sedimentary and volcanic origin.
- **preparation layer** - not always present, it is definitely thinner than the other two layers and show the presence of very fine aggregates of sedimentary origin (limestones).
- **mural painting** - it corresponds to a very tiny film of pigment painted on fresh surface. Shades of warm and cold colors were present on different samples. Sometimes, pigment is painted with no preparation layer.

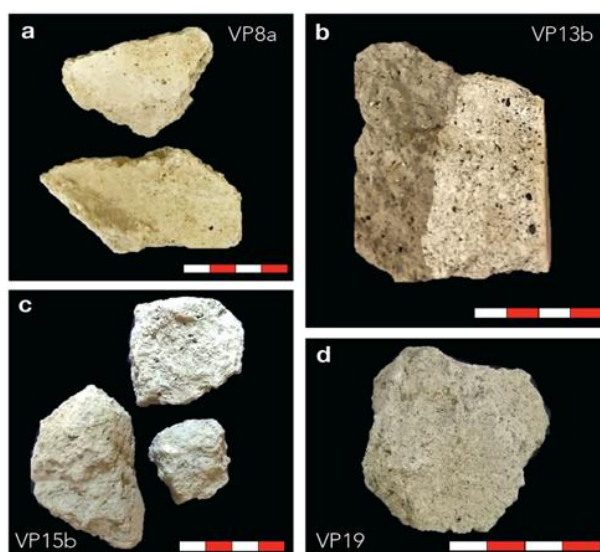


**Fig. 5.** Macroscopic pictures of plasters. (a) Sample VP8a; (b) sample VP13b; (c) sample VP15b; (d) sample VP19 (scale bar = 5 cm).

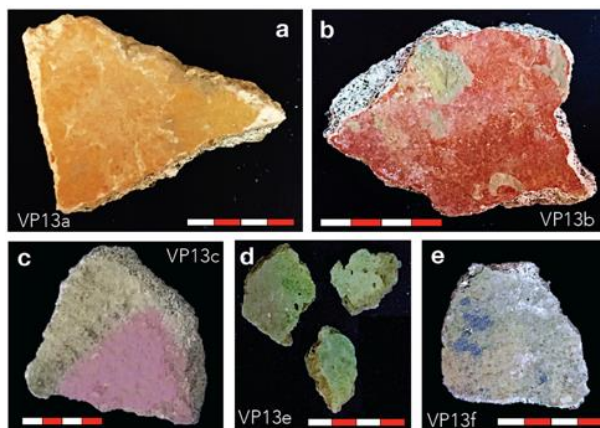


**Fig. 6.** Examples of plaster samples with fresco’s pigments. (a) Sample VP13a; (b) sample VP13b; (c) sample VP13c; (d) sample VP13e; (e) sample VP13f (scale bar = 2 cm).

Petrographic features were gathered from POM of representative samples are shown in figures 7 and 8.

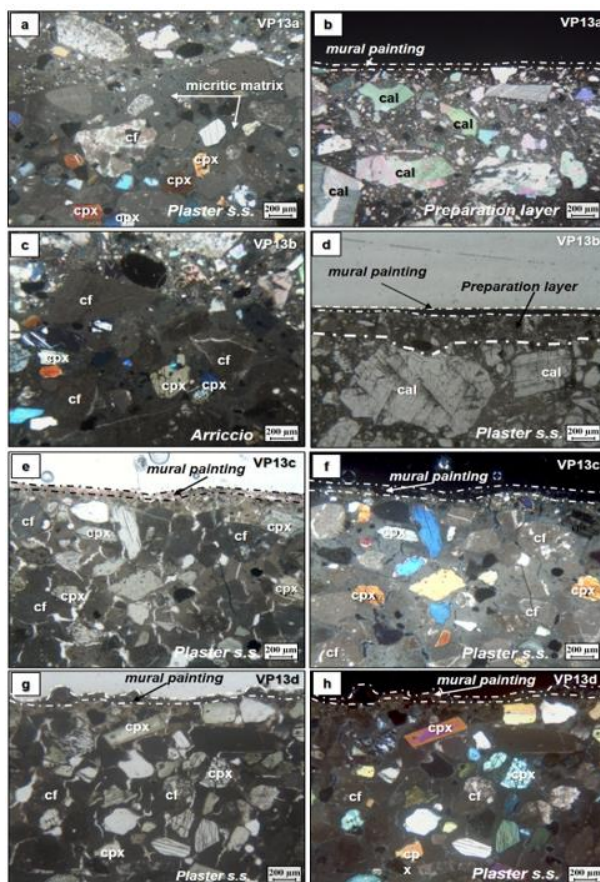


**Fig. 7.** Micrographs of plaster set VP13a-VP13d from POM observations (see text for detailed explanation). Abbreviations: cal = calcite, cpx = clinopyroxene, cf = carbonate fragment.

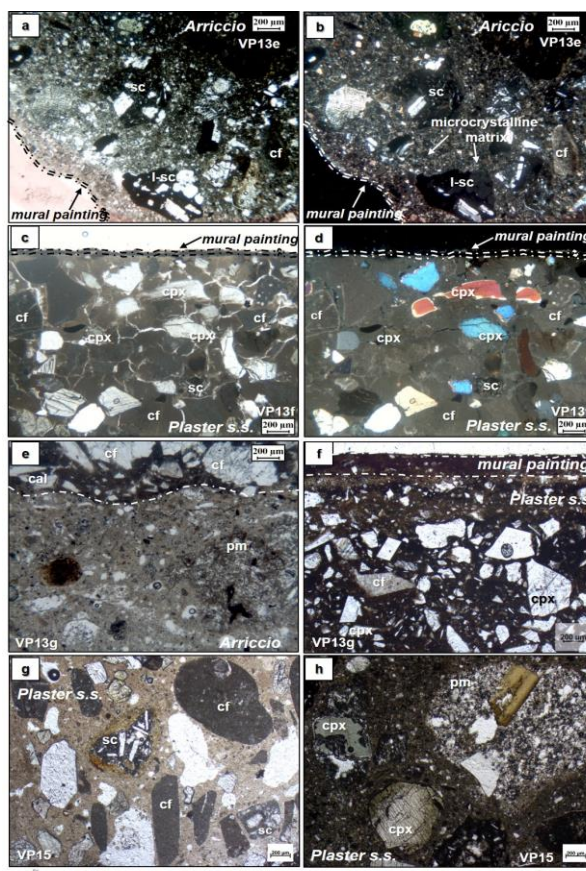


**Fig. 8.** Micrographs of plaster set VP13e-VP13f-VP13g-VP15c from POM observations (see text for detailed explanation). Abbreviations: cal = calcite, cpx = clinopyroxene, cf = carbonate fragment, sc = scoriae; l-sc= scoriae with leucite.

Plaster samples usually have different layers with always distinct transitions between them and without evidence of recarbonation process.

Plaster s.s. (Figs. 7 and 8) shows a carbonate micritic matrix and aggregates are mainly characterized by carbonate fragments, ranging in size from few millimeters to almost one centimeter; in addition, scoriae and pumices as well as clinopyroxene, alkali-feldspar and amphibole crystals occur.

Figures 7a ad 7b show sample VP13a, composed of three layers: with distinct transitions between them and with any evidence of recarbonation. The inner layer (*plaster s.s.*, Fig. 7a), shows a carbonate micritic matrix. Aggregates are mainly characterized by carbonate fragments, ranging from few millimeters to one centimeter in size, scoriae and pumices as well as clinopyroxene, alkali-feldspar and amphibole crystals.

*Preparation layer* (Fig. 7b) is present and shows a carbonate nature; it is mainly composed of a micritic groundmass, rarely cryptocrystalline, with carbonate fragments and calcite crystals. The mural painting is present with an ocher color. In figures 7c and 7d, sample VP13b shows the complete plaster stratigraphy (Table 1) of four layers (Fig. 5), with sharp transitions and no recarbonation evidences. *Arriccio* (Fig. 7c) is composed of a mainly micritic carbonate groundmass. The conglomeratic aggregates are characterized by carbonate fragments with a size of less than a millimeter, and loose crystals of clinopyroxene, alkali feldspar, amphibole and biotite. *Plaster s.s.* (Fig. 7a,d) is a carbonatic binder, mainly characterized by a

micritic to (subordinate) cryptocrystalline carbonate groundmass, with carbonate fragments and calcite crystals. The preparation layer can clearly be observed in Fig. 7d; it is composed of a carbonatic matrix binder with fine (millimetric size) limestone clasts and fragments of calcite crystals. Mural painting is represented by a deep red-colored surface (Fig. 5b and 6b).

Figures 7e and 7f (sample Vp13c, Table 1) and figures 7g and 7h (sample Vp13d, Table 1) show similar mineralogical and petrographic features, i.e. single layered samples with no preparation layer and mural painting directly on plaster s.s. The latter layer is characterized by a prevailing micritic carbonate matrix with aggregates mainly characterized by carbonate fragments of millimetric size, scoriae, and crystal fragments of clinopyroxene, alkali feldspar, amphibole and biotite. Mural paintings are respectively purple-colored (Figs. 7e,f) and blue-colored external surfaces (Figs. 7g,h). Sample VP13d shows rare garnet crystals also found in the micritic carbonate matrix.

An *arriccio* sample with a prevailing microcrystalline carbonate groundmass is shown in figures 8a and 8b (sample VP13e; Table 1); the aggregates are composed of volcanic fragments, such as pumices and scoriae with leucite, together with carbonate fragments, clinopyroxene and alkali feldspar. This sample shows the lack of preparation layer before the mural painting, which is green in color (Fig. 6d) and painted directly on the *arriccio*.

*Plaster s.s.* with external fresco surface (blue-painted) is presented in figures 8c and 8d (sample VP13f; Table 1). Sample VP13g (Figs. 8e,f and Table 1) is interesting due to occurrence of the complete stratigraphy, as defined in figure 4b; it shows a sharp transition between layers and no evidence of recarbonation process. Just like the others, *arriccio* is mainly characterized by a micritic carbonate matrix with carbonate fragments, leucite-bearing scoriae, pumices and clinopyroxene crystals. Plaster s.s. is a carbonate binder, composed of a micritic and/or cryptocrystalline matrix with sedimentary aggregates and calcite crystals. Preparation layer is very similar to the plaster s.s. but thinner and with finer aggregate size. The mural painting is present and pink/orange in color.

Figures 8g and 8h (sample VP15c, Table 1) illustrates a sample of *arriccio*; a single layer made of a prevailing microcrystalline carbonate matrix with pumice and leucite-bearing scoriae along with loose crystals of calcite, clinopyroxene, rare plagioclase and biotite. Aggregates are both rough and rounded with mainly coarse grain size (3-4 mm grains) and with only a little percentage (less than 15%) of fine grains (<0.5 mm).

The mineralogical and petrographic features of all the other *arriccio* samples of this study (VP15a, VP15b, VP16, VP17, VP18, VP19; Table 1) are quite similar and nearly comparable to sample VP15c.

An interesting approach concerning a non-destructive examination of the Positano plasters composition vs. texture is given by the  $\mu$ -CT analysis (Fig. 9).

Figures 9a and 9b points out the occurrence of pumices, represented by the blackish areas (sample 8a), whereas the whitish-grey elements correspond to pyroxene and mica crystals and medium-grey to plagioclase, all included in a dark-grey matrix. Various shades of grey are also observed in the other samples; in particular, in sample 13b both *arriccio* and *plaster s. s.* layers can be observed (Fig. 9d), with the black spots corresponding to pores. Along with black, three different shades of colour are visible and, as in the previous sample, the darkest elements are alkali feldspar and plagioclases crystals, the intermediate grey corresponds to calcite and the brighter grey elements are pyroxenes and mica crystals. Figures 9e and 9f show a bedding mortar (sample 15a), with the pores in black and pumices in darkest grey. The intermediate greys can be ascribable to the silic component, i.e. leucite and feldspar, whereas the brighter elements are pyroxene and mica. Figure 9g shows a bedding-lining mortar (sample 19), in which the majority of crystals is represented by plagioclase (darker grey), calcite (in lighter grey) and Fe-bearing mafic minerals and/or oxides (i.e. the whitish elements in figure 9g, which mainly correspond to the red ones in figure 9h).

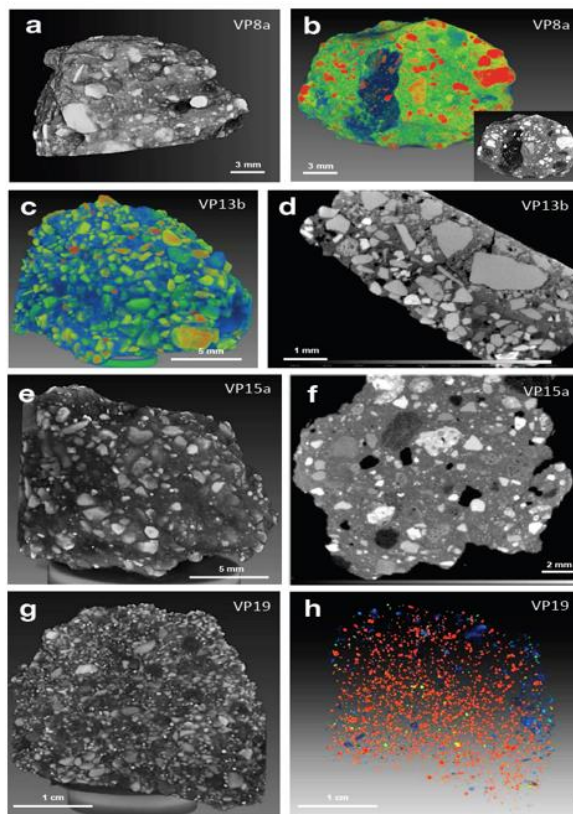


**Fig. 9.**  $\mu$ -CT images of plaster fragments from selected samples: (a,b) VP8a, (c,d) VP13b, (e,f) VP15a, (g,h) VP19.

**Table 2.** The whole mineral assemblages inferred by XRPD and SEM-EDS analyses of the studied mortar samples.

Sample ID	Mineral assemblage
VP1	Anl, Php, Afs, Pl, Cal, Mca, Px, Cbz, Lct
VP 4	Pl, Cal, Mca, Px
VP 8a	Anl, Php, Afs, Pl, Cal, Mca, Px
VP 8b	Anl, Afs, Pl, Cal, Mca, Px, Lct
VP 9	Pl, Cal, Mca, Px
VP 13a	Afs, Cal, Px, Pl, Dol, Am, Mag, Ap
VP 13b	Anl, Php, Afs, Pl, Cal, Mca, Px
VP 13c	Afs, Pl, Cal, Px, Mag, Lct, Ap
VP13d	Px, Cal, Mca
VP 13e	Anl, Php, Afs, Pl, Cal, Mca, Px, Ol, Cbz, Lct
VP 13f	Afs, Pl, Cal, Mca, Px
VP 13g	Afs, Pl, Cal, Mca, Px
VP 15a	Anl, Php, Afs, Pl, Cal, Mca, Px, Lct
VP 15b	Anl, Php, Afs, Pl, Cal, Mca, Px, Lct
VP 15c	Afs, Pl, Cal, Mca, Px, Mag
VP 16	Anl, Php, Afs, Pl, Cal, Mca, Px, Lct
VP 17	Anl, Afs, Pl, Cal, Mca, Px, Lct
VP 18	Anl, Afs, Pl, Cal, Mca, Px, Lct
VP 19	Pl, Cal, Mca, Px
VP 20	Pl, Cal, Mca, Px
VP 21	Pl, Cal, Mca, Px

Mineral abbreviations partly from [42]: Am = amphibole; Anl = analcime; Ap = apatite; Cal = calcite; Cbz = chabazite; Dol = dolomite; Afs = alkali feldspar; Lct = leucite; Mag = magnetite; Mca = mica; Php = phillipsite; Pl = plagioclase; Px = pyroxene; Ol = olivine.

The whole mineralogy was further assessed combining analytical results from XRD SEM EDS and FTIR. XRD (Table 2), SEM-EDS analyses and FTIR investigations (Fig. 10 and Table 3) confirmed that the samples are constituted by complex mixtures of variable amounts of silicates, such as feldspars, clinopyroxene, micas, leucite, zeolites (analcime, phillipsite, chabazite), carbonates (prevailing calcite and subordinate dolomite) and other trace phases (Ti-magnetite, apatite, olivine). The amorphous component, i.e. the pumice clasts occurring in some samples, can show reaction rims and dissolution phenomena, as a result of pozzolanic reaction processes (Figs. 10 b,d) as also reported by Secco et al. (2019).

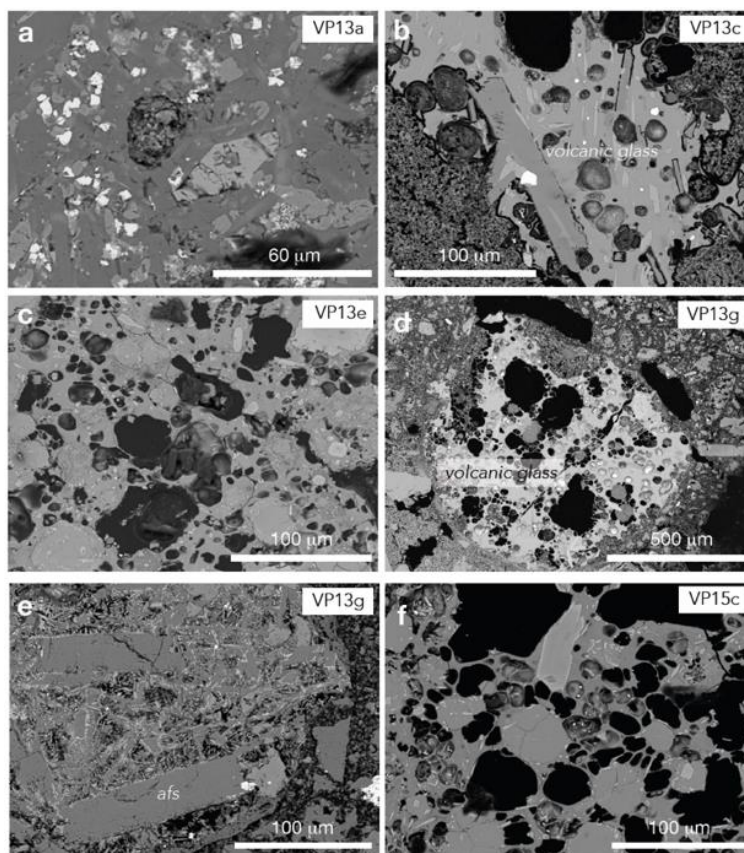


**Fig. 10.** SEM-EDS of representative plaster samples (abbreviations from [42])

Finally, a restricted set of pigments used in the color coatings (Fig. 6) were preliminarily characterized via XRPD analysis (Table 4) and range from warm to cold colors. Warm colors (red, yellow) were made using iron oxides; cold colors (blue, green) can be likely related to copper-bearing minerals. In particular, red and yellow colors are respectively obtained using hematite and goethite, i.e. the main constituents of red to yellow ochers. The green color used in the Positano's paintings is obtained by malachite, as observed by [43] as well; the blue color is derived from cuprorivaite, a Cu-Ca-bearing silicate obtained by the heating of silica, malachite, calcium and sodium carbonates or following different recipes [44].

Table 3 shows selected chemical compositions of the dominant minerals forming the mortar artefacts, as well as the glass components.

**Table 3.** Selected chemical composition of minerals and volcanic glass fractions detected in studied samples.

	feldspar								leucite	
	VP13a	VP13a	VP13c	VP13g	VP13g	VP13g	VP13g	VP15c	VP13e	VP13e
SiO <sub>2</sub>	63.68	54.97	50.44	64.73	50.52	46.26	61.23	47.61	56.75	55.36
TiO <sub>2</sub>	0.00	0.00	0.28	0.00	0.00	0.00	0.00	0.00	0.07	0.00
Al <sub>2</sub> O <sub>3</sub>	18.57	27.89	29.61	20.05	30.28	34.95	21.90	33.20	22.97	23.35
FeO <sub>t</sub>	0.26	0.65	1.77	0.91	0.46	0.49	1.55	0.92	0.62	0.68
MgO	0.00	0.00	0.49	0.00	0.00	0.00	0.00	0.04	0.00	0.05
CaO	0.00	10.11	13.05	0.66	12.50	17.28	3.16	15.27	0.02	0.10
Na <sub>2</sub> O	0.33	5.50	2.62	5.28	3.37	1.56	7.52	2.26	0.33	0.69
K <sub>2</sub> O	15.58	0.87	1.85	8.89	0.71	0.00	3.93	0.56	19.47	19.46
SrO	1.49	0.35	0.00	0.17	1.12	0.00	0.11	0.00	0.00	0.00
BaO	0.00	0.00	0.00	0.02	0.75	0.00	0.36	0.00	0.00	0.00
Total	99.91	100.35	100.11	100.70	99.71	100.54	99.75	99.86	100.23	99.69
	clinopyroxene				mica		olivine			
	VP13a	VP13c	VP13e	VP15c	VP15c	VP15c	VP13e	VP13e		
SiO <sub>2</sub>	48.44	53.28	44.01	52.38	38.20	34.49	38.21	38.08		
TiO <sub>2</sub>	1.19	0.37	1.95	0.69	2.30	3.07	0.00	0.02		
Al <sub>2</sub> O <sub>3</sub>	6.48	1.35	8.51	3.31	15.46	16.38	0.22	0.24		
Cr <sub>2</sub> O <sub>3</sub>	0.00	0.18	0.00	0.00	0.00	0.00	0.00	0.26		
FeO <sub>t</sub>	8.30	3.49	9.98	4.24	6.15	11.17	25.13	22.57		
MnO	0.17	0.00	0.00	0.38	0.00	0.02	0.27	0.34		
MgO	12.68	16.93	9.95	15.80	20.46	16.22	36.25	37.86		
CaO	22.21	23.92	22.18	23.66	0.22	0.27	0.28	0.36		
Na <sub>2</sub> O	0.25	0.11	1.15	0.22	0.18	0.33	0.16	0.05		
K <sub>2</sub> O	0.00	0.00	0.14	0.00	9.40	9.02	0.04	0.00		
BaO	0.00	0.00	0.00	0.00	0.53	1.28	0.00	0.00		
F	0.00	0.00	0.00	0.00	0.59	0.00	0.00	0.00		
Total	99.72	99.63	97.88	100.69	93.50	92.25	100.56	99.78		
	dolomite		calcite		apatite		spinel			
	VP13a	VP13a	VP15c	VP15c	VP13a	VP13a	VP13a	VP15c		
SiO <sub>2</sub>	0.00	0.00	0.04	0.01	0.08	0.24	1.89	0.67		
TiO <sub>2</sub>	0.00	0.00	0.00	0.00	0.00	5.55	6.26	21.29		
Al <sub>2</sub> O <sub>3</sub>	0.00	0.00	0.03	0.00	0.11	0.71	1.89	2.32		
FeO <sub>t</sub>	0.00	0.00	0.15	0.05	0.44	79.80	76.63	69.98		
MnO	0.00	0.00	0.00	0.00	0.00	2.24	1.52	1.44		
MgO	18.52	0.00	0.00	0.00	0.00	1.72	1.14	0.45		
CaO	29.94	51.58	51.13	51.55	52.78	0.16	0.33	0.12		
Na <sub>2</sub> O	0.00	0.00	0.00	0.07	0.12	0.00	0.00	0.00		
K <sub>2</sub> O	0.00	0.00	0.00	0.00	0.00	0.00	0.00	0.00		
SrO	0.00	0.00	0.00	0.00	0.73	0.00	0.00	0.00		
P <sub>2</sub> O <sub>5</sub>	0.00	0.00	0.00	0.00	38.21	0.00	0.00	0.00		
As <sub>2</sub> O <sub>5</sub>	0.00	0.00	0.00	0.00	0.26	0.00	0.00	0.00		
La <sub>2</sub> O <sub>3</sub>	0.00	0.00	0.00	0.00	0.19	0.00	0.00	0.00		
Nd <sub>2</sub> O <sub>3</sub>	0.00	0.00	0.00	0.00	0.94	0.00	0.00	0.00		
Cl	0.00	0.00	0.00	0.00	0.38	0.00	0.00	0.00		
Total	48.46	51.58	51.34	51.68	94.24	90.43	89.66	96.28		
	volcanic glass									
	VP13c	VP13c	VP13e	VP13e	VP13e	VP13g	VP13g	VP15c		
SiO <sub>2</sub>	51.17	50.80	55.03	54.61	52.42	48.17	48.76	53.08		
TiO <sub>2</sub>	0.79	0.65	0.34	0.54	0.62	0.75	0.91	0.31		
Al <sub>2</sub> O <sub>3</sub>	17.73	17.93	21.54	20.82	19.71	19.44	19.77	20.04		
FeO <sub>t</sub>	6.98	6.12	2.79	3.09	2.94	6.10	6.64	3.27		
MnO	0.35	0.22	0.18	0.40	0.07	0.40	0.61	0.11		
MgO	1.45	1.45	0.05	0.16	0.25	1.51	1.81	0.39		
CaO	5.62	5.94	2.92	2.62	3.63	7.95	7.67	4.12		
Na <sub>2</sub> O	2.80	3.13	6.78	5.83	6.75	3.72	3.40	6.38		
K <sub>2</sub> O	7.80	7.21	5.89	8.02	5.77	7.42	7.19	7.22		
Cl	0.63	0.83	0.87	1.00	0.86	0.56	0.51	0.86		
Total	95.33	94.27	96.40	97.10	93.05	96.00	97.27	95.80		

**Table 4.** Mineralogical composition of pigments in the studied samples inferred by XRPD.

Color	Minerals
yellow	goethite FeO(OH)
red	hematite Fe <sub>2</sub> O <sub>3</sub>
orange	goethite, hematite
pink	hematite, calcite CaCO <sub>3</sub>
green	malachite Cu <sub>2</sub> (CO <sub>3</sub> )(OH) <sub>2</sub>
blue	cuprorivaite CaCuSi <sub>4</sub> O <sub>10</sub>

*Roof tiles*

The studied roof tiles (Fig. 11) have been mainly distinguished at a mesoscopic scale by color and structure in four types labelled VP12a, VP12b, VP12c, and VP12d. From a macroscopic point of view, they are characterized by colors [45] slightly varying from yellow (10YR 7/6; VP12a), reddish yellow (7.5YR 6/6; VP12b, VP12d) to yellowish red (5YR 5/8; VP12c).

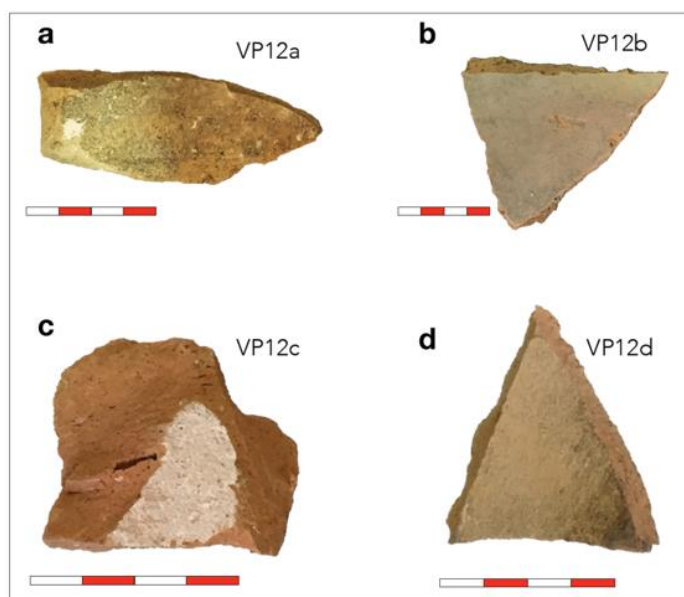


**Fig. 11.** Macroscopic photos of roof tiles. (a) VP12a; (a) VP12b; (a) VP12c; (a) VP12d (scale bar = 5 cm).

Observed with POM, sample VP12a (Figs. 12a,b) shows an isotropic matrix. Inclusions approximately range from 20 to 30% and show a bimodal distribution with a siliciclastic fine fraction. Coarser grains ( $\approx 100\text{-}200\ \mu\text{m}$ ) are mostly composed of crystals of clinopyroxene, alkali feldspar, and minor garnet, biotite, and olivine; volcanic glass and scoriae with plagioclase and leucite, basalt- and leucitite-derived respectively, also occur. Carbonate fragments are frequent and mostly decomposed, often showing voids left from decomposition with reaction rims on the surfaces [46]; microcrystalline calcite is widespread in the matrix (b-fabric; [47]) due to re-carbonation [46] or occurs as secondary phase on the surfaces of voids.

Sample VP12b (Fig. 12c) shows an active matrix. Inclusions (10-20%) are mainly represented by coarse pumices, volcanic scoriae containing alkali feldspar (trachytic composition; [48]), clinopyroxene, plagioclase, and biotite; rare clasts of decomposed carbonate are also present. Very peculiar is the presence of a large amount of tiny volcanic glass shards in the matrix.

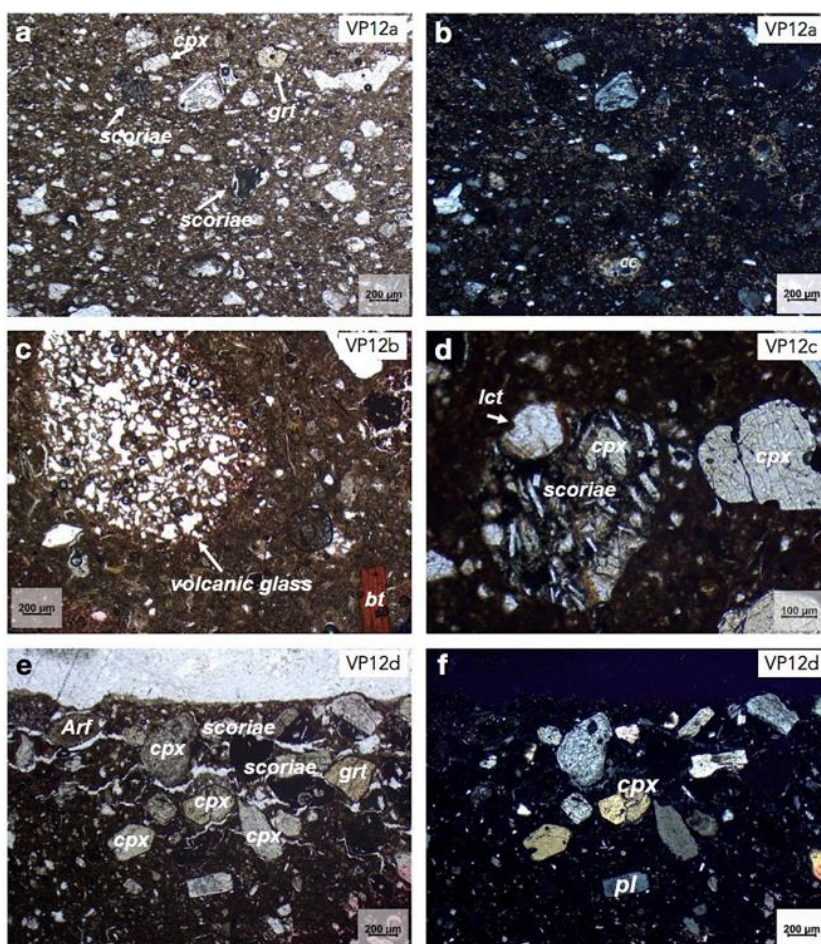


Fig.12. POM micrographs of roof tiles (abbreviations partly from [42]).

Sample VP12c (Fig. 12d) shows a weakly active matrix with microcrystalline calcite is widespread in the matrix and in the pores. Inclusions (20-30%) show a bimodal distribution. The finer fraction is represented by siliciclastic crystals. Coarser grains are mostly clinopyroxene and alkali feldspar, with minor plagioclase, garnet and biotite. Scoriae and volcanic glass were also found, along with rare crystals of plagioclase and leucite. Occasional decomposed carbonate clasts were also observed.

Sample VP12d (Figs. 12e,f) shows an isotropic matrix. Inclusions range between 20 and 30% and show a bimodal distribution. The grains in this sample show a peculiar arrangement characterized by a higher packing along the margins of the fragment. Inclusions are characterized by a finer siliciclastic fraction and coarser grains composed of clinopyroxene and alkali feldspar, along with minor amounts of plagioclase, garnet, and biotite; scoriae, volcanic lithics, and leucite were also found occur. Secondary microcrystalline calcite in the matrix and on pores surface also occur in low amounts. The occurrence of mainly elongated pores (darker areas) can be clearly observed in the  $\mu$ -CT images of figure 13.

Observed at SEM-EDS (Fig. 14a), the tile samples confirm their very heterogeneous textures. Minor (i.e Fe-oxides, magnetite and other iron-bearing phases) to trace minerals (i.e. apatite, amphibole) were further detected, if compared to the POM. Glass fraction is commonly present (see for instance Fig. 14c,e,g,k); tiny inclusions of Fe-oxides can be found at the

boundaries between clinopyroxenes and glass, such as in sample VP12d (Fig. 14l). Table 5 summarizes the mineralogical components detected in the roof tiles deduced by POM and SEM-EDS investigations, whereas Table 6 shows selected chemical compositions of the dominant minerals and glass components found in these samples. It is interesting to note, for instance, that garnets correspond to a solid solution of prevailing andradite and subordinate grossular [49].

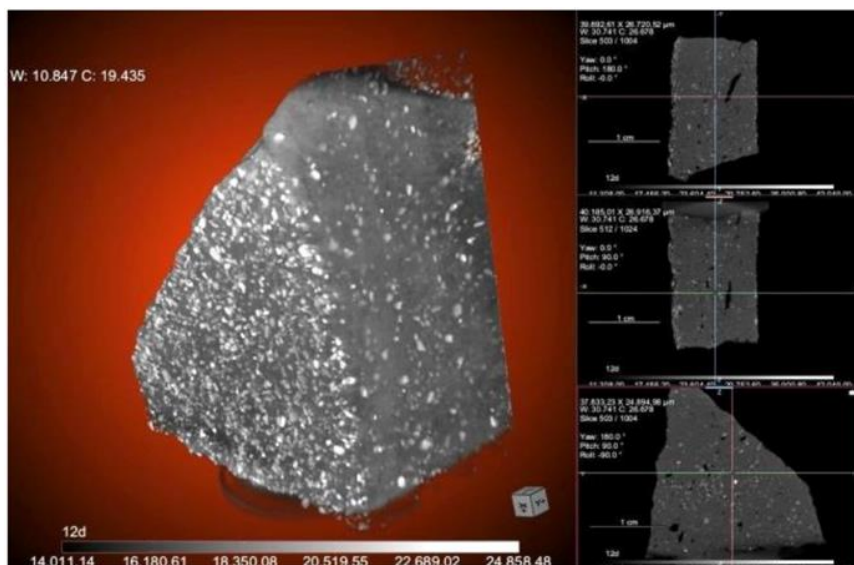


Fig. 13. μ-CT images of sample VP12d.

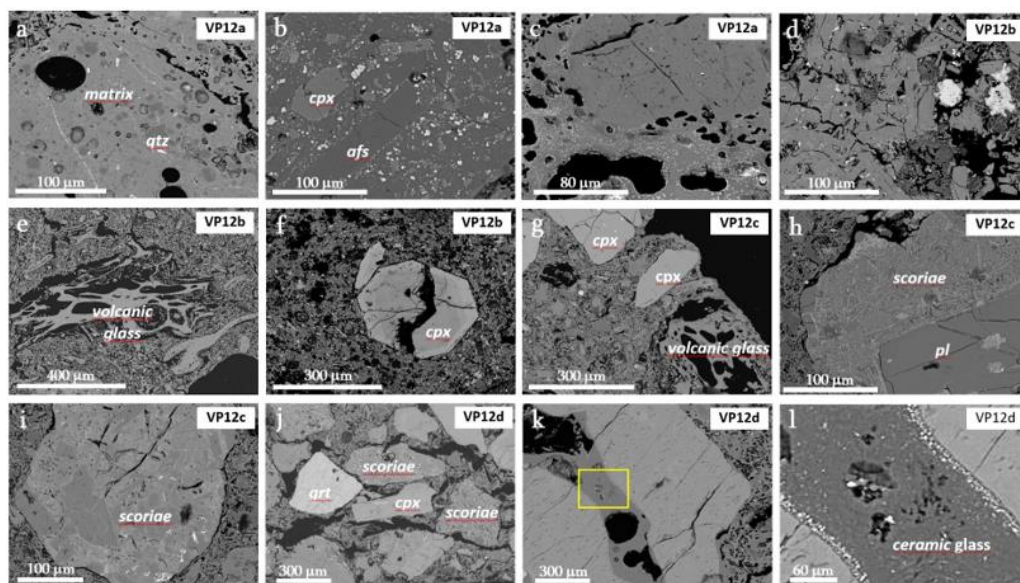


Fig. 14. SEM-BSE micrographs of the investigated Positano villa's tiles (see text for further explanation). (a,b,c) Sample VP12a; (d,e,f) sample VP12b; (g,h,i) sample VP12c; (j,k) sample VP12; (l) enlargement of the area in the yellow frame of (k) (abbreviations partly from [42])

**Table 5.** Mineralogical composition of the Positano villa's tiles inferred by POM and SEM-EDS

Sample ID	Main components
VP 12a	Afs, Pl, Qz, Cpx, Lct, Bt, Fe-ox, Grt, Ap, Pm, Sc
VP 12b	Afs, Pl, Cpx, Qz, Fe-ox, Bt, Grt, Ap, Pm, Sc
VP 12c	Afs, Pl, Qz, Cpx, Cal, Bt, Fe-ox, Amph, Lct, Ap, Pm, Sc
VP 12d	Afs, Pl, Cal, Cpx, Qz, Fe-ox, Bt, Grt, Lct, Pm, Sc

(abbreviations: Amph = amphibole; Ap = apatite; Bt = biotite; Cal = calcite; Cpx = clinopyroxene; Fe-ox = Fe oxy-hydroxides; Afs = alkali feldspar; Grt = garnet; Lct = leucite; Pl = plagioclase; Pm = pumice; Qz = quartz; Sc = scoria).

**Table 6.** Selected chemical composition of minerals and volcanic glass fractions detected in the roof tiles.

	feldspar											
	VP12a	VP12a	VP12a	VP12a	VP12a	VP12b	VP12b	VP12b	VP12c	VP12c	VP12c	VP12c
SiO <sub>2</sub>	49.59	48.34	61.65	58.91	62.12	61.65	58.91	62.12	64.95	64.58	47.08	49.26
Al <sub>2</sub> O <sub>3</sub>	31.22	31.35	19.96	21.38	19.30	19.96	21.38	19.30	18.97	18.48	35.23	32.45
FeO <sub>t</sub>	0.91	0.69	0.61	4.60	3.36	0.61	4.60	3.36	0.00	0.00	0.00	0.65
CaO	13.61	13.93	1.00	0.94	1.03	1.00	0.94	1.03	0.17	0.25	16.78	13.98
Na <sub>2</sub> O	2.86	2.83	2.79	4.38	3.68	2.79	4.38	3.68	1.95	1.44	1.47	2.67
K <sub>2</sub> O	0.73	0.93	11.07	8.61	8.69	11.07	8.61	8.69	13.96	13.86	0.19	0.64
SrO	0.43	0.99	0.12	0.00	0.34	0.12	0.00	0.34	0.00	0.00	0.00	0.40
BaO	0.99	0.62	2.58	0.00	0.62	2.58	0.00	0.62	0.00	0.24	0.00	0.84
Total	100.36	99.67	99.79	98.82	99.13	99.79	98.82	99.13	100.00	98.85	100.75	100.88
	clinopyroxene				mica		amphibole		garnet			
	VP12b	VP12b	VP12b	VP12c	VP12a	VP12c	VP12b	VP12b	VP12b	VP12b	VP12b	VP12b
SiO <sub>2</sub>	43.41	50.76	45.21	48.55	30.07	36.60	34.46	35.11	36.91			
TiO <sub>2</sub>	1.60	0.63	1.71	0.81	0.08	2.26	0.00	0.25	0.06			
Al <sub>2</sub> O <sub>3</sub>	10.79	4.37	8.06	5.35	18.50	14.94	0.19	0.17	6.35			
Cr <sub>2</sub> O <sub>3</sub>	0.16	0.00	0.17	0.06	0.00	0.00	0.38	0.22	0.28			
FeO <sub>t</sub>	8.12	5.68	8.80	7.91	24.05	23.02	29.23	29.24	21.71			
MnO	0.27	0.13	0.55	0.32	0.35	0.41	0.03	0.27	0.23			
MgO	11.26	15.14	10.99	12.81	12.21	5.42	0.16	0.14	0.49			
CaO	21.57	23.44	23.19	22.23	0.13	10.85	31.87	31.23	33.31			
Na <sub>2</sub> O	0.07	0.34	0.38	0.19	0.81	1.40	0.07	0.30	0.22			
K <sub>2</sub> O	0.00	0.00	0.00	0.00	3.95	2.42	0.00	0.00	0.00			
SrO	0.00	0.00	0.00	0.00	0.34	0.00	0.00	0.00	0.00			
F	0.00	0.00	0.00	0.00	0.00	1.27	0.00	0.00	0.00			
Cl	0.00	0.00	0.00	0.00	0.01	0.37	0.00	0.00	0.00			
Total	97.25	100.49	99.06	98.21	90.49	98.96	96.39	96.93	99.56			
	Ti-magnetite		apatite		volcanic glass							
	VP12a	VP12a	VP12a	VP12a	VP12a	VP12a	VP12b	VP12b	VP12c	VP12c	VP12c	VP12c
SiO <sub>2</sub>	0.94	1.02	62.08	61.94	62.31	59.09	62.11	63.56	63.74	63.38	60.74	
TiO <sub>2</sub>	7.42	0.00	0.16	0.39	0.00	0.09	0.45	0.70	0.37	0.49	0.29	
Al <sub>2</sub> O <sub>3</sub>	5.80	0.63	21.20	18.30	19.33	21.34	19.22	19.66	19.75	19.37	18.67	
FeO <sub>t</sub>	70.02	0.71	0.59	0.00	1.47	4.59	3.36	1.39	1.41	2.93	2.23	
MnO	0.16	0.28	0.00	0.06	0.15	0.35	0.30	0.10	0.00	0.31	0.00	
MgO	5.58	0.00	0.00	0.00	0.39	0.45	0.32	0.37	0.47	0.72	0.11	
CaO	0.39	51.24	3.36	0.39	5.05	0.94	1.03	1.96	1.85	2.76	1.33	
Na <sub>2</sub> O	0.00	0.28	2.67	1.04	1.80	4.35	3.66	3.23	2.78	2.74	2.90	
K <sub>2</sub> O	0.00	0.15	9.40	13.71	5.15	8.61	8.70	8.16	8.11	7.57	7.80	
SrO	0.00	0.48	0.00	0.00	0.00	0.00	0.00	0.00	0.00	0.00	0.00	
P <sub>2</sub> O <sub>5</sub>	0.00	38.67	0.00	0.00	0.00	0.00	0.00	0.00	0.00	0.00	0.00	
La <sub>2</sub> O <sub>3</sub>	0.00	0.38	0.00	0.00	0.00	0.00	0.00	0.00	0.00	0.00	0.00	
Ce <sub>2</sub> O <sub>3</sub>	0.00	0.32	0.00	0.00	0.00	0.00	0.00	0.00	0.00	0.00	0.00	
Nd <sub>2</sub> O <sub>3</sub>	0.00	0.43	0.00	0.00	0.00	0.00	0.00	0.00	0.00	0.00	0.00	
F	0.00	0.38	0.00	0.00	0.00	0.00	0.00	0.00	0.00	0.00	0.00	
Cl	0.00	0.66	0.00	0.15	0.00	0.06	0.00	0.00	0.00	0.05	0.00	
Total	90.31	95.64	99.45	95.97	95.66	99.87	99.15	99.13	98.49	100.31	94.08	

**The geoarcheological reconstruction**

The *otium villae* of the Amalfi Coast (Fig. 2), which first overcome by the fallout material and immediately afterwards by the violence of the flow-slides related to the AD 79 plinian eruption, have provided information for the reconstruction of the ancient landscape [19]. The AD 79 eruption buried and preserved Pompeii, Herculaneum and Stabia and their inhabitants, but also the maritime villas, as well as farms, irrigation canals and aqueducts, orchards and vineyards, ports, etc. [50]. Even extremely transient objects were preserved; for instance, at Positano it is worth noting the imprint of a textile cover (*Velarium*) (Fig. 15a).

The eruption triggered secondary, equally destructive events, that overwhelmed coastal areas, plains and mountains: volcanoclastic mudflows, deviation of river courses. Pumice and ash floated for years along the Campania coast. The port of Naples itself was seriously damaged, as other areas of the Salerno gulf; Pompeii lies buried at about two kilometers from the present-day coastline. Hence, the whole of the complex events triggered by the eruption significantly altered the landscape, much more than we had previously thought.

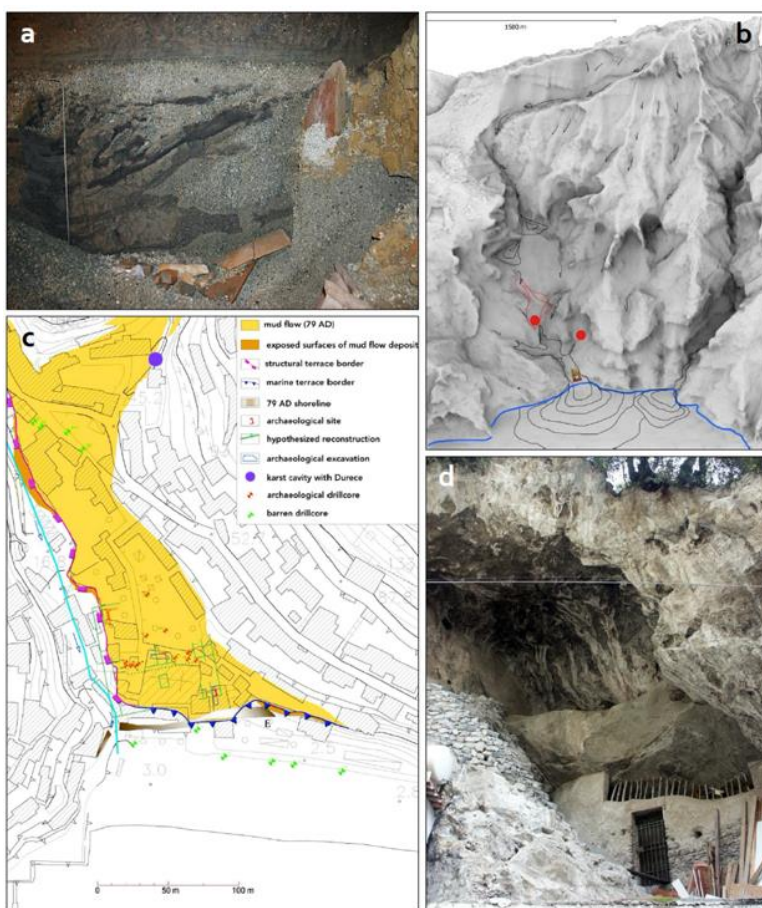


**Fig. 15.** (a) Convolutions and laminations highlighted by granulometric changes within the succession of collapses in the triclinium, likely attributable to variations in facies caused by the presence of the large *Velarium*-type covers (Geomed Archive); (b) DTM model Porto Valley with the location of the volcanoclastic flow lobes and of the invaded karst cavities (Geomed Archive); (c) geoarchaeological structure of the volcanoclastic lobe of A. D. 79 deposits in Positano (Geomed Archive); (d) karst cavity with internal lobe of volcanoclastic “*Durece*” at Positano (photo by G. Di Maio).

At Positano, in the Porto valley a little less than two meters of pumice and ash fell (Figs. 15b,c). It can be hypothesized that in that stage there were no victims because the temperature was no longer high. But at least two meters of loose and extremely reactive material spread over the steep limestone walls of the Lattari Mountains could not remain in equilibrium for very long (Figs. 15b,c). The heavy rains, always associated with eruptions, activated mud avalanches, that grew bigger as they moved towards the low valley at the same time as accumulating more flows from the lateral valleys. The volcanoclastic mudflow reached a thickness of twenty meters by the time it reached the low valley, hence for the villa there was no escape.

Then, the muddy accumulation quickly consolidated, turning into the hard material of the *Durece* (Fig. 15d; see also “Geological and archaeological outline”). Information from the geoarchaeological excavations/drillcores indicates that the *Posides* villa was first affected by a thin layer of ash, then immediately by a rain of pumice that covered it up to two meters. The pitched roof of the *triclinium* helped the pumice to slide outwards. Only small quantities of pumice entered through the doors and windows. After a few hours, the same material that fell on the mountains began to slide down as an avalanche of mud. These “lahars” must have been moving at high speed when they reached the north peristyle of the villa, filling the rooms and beginning to push and rise against the same northern wall. Parts of the wooden structures of the roofs and ceilings collapsed, suspended vertically above the furniture and the furnishings. Other lobes of the flow traveled around the obstacle, reached the south *peristyle* and flowed uphill again; the lobes knocked down some of the *stucco porticus* columns and dragged one into the *triclinium*, piling up and crushing against the north wall the wooden material of the ceiling coffers, the partitions and the same scaffolding for the restorations that were in progress. Under the pressure of the increasingly heavy accumulation of mud, the walls of the *triclinium* began to collapse until the western one broke into fragments [19].

On the basis of the geoarchaeological reconstruction (Fig. 15c), the extent of the archaeological complex intrudes in depth into the footprint of the monumental structures of the S.M. Assunta church, as well as into many nearby buildings and part of the complex of the Hotel Murat. The re-incision of the Porto valley had apparently led to the erosion of part of the eastern edges of the Roman villa. These edges were the parts most exposed to the repeated spoliation that went on there since Late Antiquity [19].

## Conclusions

The archaeometric analyses of various type of samples from the luxury villa in Positano and the geoarchaeological investigations allowed us to identify their composition and to obtain basic information about the production ways and the raw geomaterials employed for the artefacts and to point out some distinctive remarks:

(i) the analyzed plasters are mainly lime-based, usually with the addition of an aggregate. The *arriccio* is made by a volcanic component, characterized by clinopyroxene, alkali feldspar, garnet, amphibole, biotite and leucite crystals, together with a sedimentary component represented by carbonate fragments, also with traces of microfossils. The source area of volcanic fractions perfectly fit into volcanic materials from Somma-Vesuvius volcanic complex [48] (and references therein), as testified by the occurrence of garnet, leucite and pumices with a mainly tephriphonolitic composition ( $\text{SiO}_2 = 48.17\text{-}55.03$  wt%;  $\text{Na}_2\text{O}+\text{K}_2\text{O} = 10.34\text{-}13.85$  wt%). Concerning the carbonate fractions recognized in the studied artefacts and the lime used in the preparation, a clear indication about the geological source area(s) cannot be given, even if a local provenance is presumable [7]. These materials show the same type of volcanic aggregates observed in the studied samples, with minor amounts of sedimentary fractions, allowing for the location of the areas nearby the villa as the most probable supply regions.

Plasters are also lime-based, but with the addition of carbonate aggregates only, in agreement with the description of Vitruvius’s “*De Architectura* (VII, 3)”; this text reported that the external layer was often formed by pure lime, carefully smoothed. If mortars substituted lime, the sands were refined or replaced by limestone parts, gypsum and powdered marble. As

also noted by [51] for similar specimens sampled in the villa, the materials used (lime, pozzolan) as well as the microstructure of the material are comparable with similar artefacts from Pompeii, Herculaneum and other Roman sites in Campania region [2,52,53]. In agreement with [51] (and references therein), the features of plasters confirm the high degree of technological standardization of masonry plasters in classical Roman age.

(ii) The mineral components recognized by preliminary XRD in the painted surfaces are mainly iron-based for the ochers-red- crimson colors and copper-based for green-blues colors. [43] also detected traces of As and Pb in some pigments (reds) of the villa, demonstrating that these materials are complex mixtures involving the use of minium and realgar/orpiment as well.

(iii) In the roof tiles two kind of tempers were identified. As regards samples VP12a, VP12c and VP12d, a volcanic temper was identified, and represented by clinopyroxene, feldspar, garnet and leucite, whereas the temper of VP12b sample contained pumices with minor amounts of alkali feldspar, clinopyroxene and biotite. In the first type of temper, the presence of both calcic garnet and leucite-bearing rock fragments indicated a provenance related to products of the Somma-Vesuvius volcano [48] (and references therein). Hence, as regards samples VP12a, VP12c and VP12d, a temper genetically related to Somma volcanic products suggested a local supplying of raw materials. Concerning the second type of temper, essentially made by trachytic pumices ( $\text{SiO}_2 = 59.09\text{-}63.74$  wt%;  $\text{Na}_2\text{O}+\text{K}_2\text{O} = 10.31\text{-}12.96$  wt.%), the source areas of volcanic raw materials can be attributable to Phlegraean Fields [48] (and references therein). The coeval occurrence of roof tiles with Vesuvian and Phlegraean tempers suggests a wide circulation in the bay of Naples of natural components but also a good production with local raw materials.

(iv) The stratigraphic data from the coring in various sites of the investigated area have shown the presence of other rooms paved in small tesserae black-and-white mosaics under at least two locations in the town, i.e. both under the Piazza Flavio Gioia and the little piazza of the Rampa Teglia (see the geoarchaeological section of Fig. 1c). Taking into account the large amount of frescoed plaster found throughout the layers of collapse and the buried material on top of them, it can be inferred that more richly frescoed rooms exist in Positano [19].

Finally, the whole dataset presented in this work can further contribute in mapping the potential extension of the archeological complex and planning recovery, restoration and conservation interventions in those parts of the site that will be possibly unearthed in the future.

## **Acknowledgments**

The Authors thank the Soprintendenza Archeologica della Campania for allowing the study of the Positano villa. Dr. R. de Gennaro and V. Monetti (DiSTAR, Università di Napoli Federico II) are respectively thanked for the technical support at the SEM-EDS and for sample preparation. This work has been funded by DiSTAR grants.

## **References**

- [1] C. Rispoli, A. De Bonis, R. Esposito, S.F. Graziano, A. Langella, M. Mercurio, V. Morra, P. Cappelletti, *Unveiling the secrets of Roman craftsmanship: mortars from Piscina Mirabilis (Campi Flegrei, Italy)*, **Archaeol Anthropol. Sci.** **12**, 2020. doi:10.1007/s12520-019-00964-8.
- [2] C. Rispoli, S.F. Graziano, C. Di Benedetto, A. De Bonis, V. Guarino, R. Esposito, V. Morra, P. Cappelletti, *New insights of historical mortars beyond pompeii: The example of Villa del Pezzolo, Sorrento Peninsula*, **Minerals** **9**, 2019. doi:10.3390/min9100575.
- [3] A. Renzulli, P. Santi, G. Balassone, G. Di Maio, A. De Bonis, V. Di Donato, V. Morra, *Trachy-phonolite lava pebbles used in the ancient settlement of oplontis (Torre annunziata, naples): Petrochemical data supporting the origin from an old effusive activity of the Somma-Vesuvius volcano*, **Ann. Geophys.** **61**, 2018, pp. 1–15. doi:10.4401/ag-7672.
- [4] G. Balassone, M. Mercurio, C. Germinario, C. Grifa, I.M. Villa, G. Di Maio, S. Scala, R.

- de' Gennaro, C. Petti, M.C. Del Re, M.C. Del Re, A. Langella, *Multi-analytical characterization and provenance identification of protohistoric metallic artefacts from Picentia-Pontecagnano and the Sarno valley sites, Campania, Italy*, **Measurements**, **128** 2018, 104–118. doi:10.1016/j.measurement.2018.06.019.
- [5] C. Di Benedetto, S.F. Graziano, V. Guarino, C. Rispoli, P. Munzi, V. Morra, P. Cappelletti, *Romans' established skills: mortars from D46b Mausoleum, Porta Mediana Necropolis, Cuma (Naples)*, **Mediterr. Archaeol. Archaeom.** **18**, 2018. pp. 131–146. doi:10.5281/zenodo.1285895.
- [6] S.F. Graziano, C. Di Benedetto, V. Guarino, C. Rispoli, P. Munzi, P. Cappelletti, V. Morra, *Technology and building materials in Roman age (1st BC - 2nd AD): The "Mausoleo Della Sfinge" from the archaeological site of Cuma (Italy)*, **Mediterr. Archaeol. Archaeom.** **18**, 2018, pp. 81–94. doi:10.5281/zenodo.1256057.
- [7] V. Morra, A. De Bonis, C. Grifa, A. Langella, L. Cavassa, R. Piovesan, *Minero-petrographic study of cooking ware and pompeian red ware (Rosso Pompeiano) from Cuma (Southern Italy)*, **Archaeometry** **55**, 2013, pp. 852–879. doi:10.1111/j.1475-4754.2012.00710.x.
- [8] C. Grifa, V. Morra, A. Langella, P. Munzi, *Byzantine ceramic production from Cuma (Campi Flegrei, Napoli)*, **Archaeometry** **51**, 2009, pp. 75–94. doi:10.1111/j.1475-4754.2008.00416.x.
- [9] C. Grifa, A. De Bonis, A. Langella, M. Mercurio, G. Soricelli, V. Morra, *A Late Roman ceramic production from Pompeii*, **J. Archaeol. Sci.** **40**, 2013, pp. 810–826. doi:10.1016/j.jas.2012.08.043.
- [10] C. Grifa, A. De Bonis, V. Guarino, C.M. Petrone, C. Germinario, M. Mercurio, G. Soricelli, A. Langella, V. Morra, *Thin walled pottery from Alife (Northern Campania, Italy)*, **Period. Mineral.** **84**, 2015, pp. 65–90. doi:10.2451/2015PM0005.
- [11] V. Guarino, A. De Bonis, C. Grifa, A. Langella, V. Morra, L. Pedroni, *Archaeometric study on terra sigillata from Cales (Italy)*, **Period. Di Mineral.** **80** (2011) 455–470. doi:10.2451/2011PM0030.
- [12] A. Campanelli, G. Di Maio, R. Iaccarino, M.A. Iannelli, L. Jacobelli, *The Roman Villa of Positano*, in: A. Marzano, G. Metraux (Eds.), *Rom. Villas or Near Bay Naples Marit. Villas, Part I*, **Cambridge University Press**, 2018, pp. 120–124. doi:10.1017/9781316687147.009.
- [13] J.H. D'Arms, *Romans on the Bay of Naples and other essays on Roman Campania*, reprint of, Zevi F. Ed, Edipuglia, Bari, 2003.
- [14] M. Della Corte, *Posides Claudii Caesaris libertus - Positano da Posidetanum?* In: **Riv. Indo-Greca-Italica** **20**, 1936, pp. 67–73.
- [15] P. Mingazzini, *Positano (prov. di Salerno) - Resti di una villa romana presso la Marina*, in: **NSc VII, Fasc. IX**, 1931, pp. 356–359.
- [16] P. Mingazzini, F. Pfister, *Formae Italiae. Regio I Latium et Campania, Vol. II Surrentum*, **Florence**, 1946.
- [17] A. Maiuri, *Le vicende dei monumenti antichi della costa amalfitana e sorrentina alla luce delle recenti alluvioni*, In: **Rend. Acc. Arch. Lett. Belle Arti Napoli**, **XXIX**, 1955, pp. 87–98.
- [18] G. Di Maio, L. Jacobelli, M.A. Iannelli, G. Balassone, *Nella villa Romana di Positano*, **Archeol. Viva Ed. Giunti**, 2017, pp. 8–19.
- [19] G. Di Maio, M.A. Iannelli, *Positano and the Roman villas of the Amalfi Coast. The archaeological landscape and the effects of the Pliny eruption of 79 AD*, in: **Leisure Villa, MAR Positano, Operaedizioni Salerno**, 2019, pp. 132–161.
- [20] G. Balassone, P. Cappelletti, G. Di Maio, A. De Bonis, C. Di Benedetto, S.F. Graziano, V. Guarino, V. Morra, C. Rispoli, *The Roman villa of Positano: preliminary mineralogical and petrographic data on archaeological findings*, in: **LeisureVilla, MAR Positano, Operaedizioni Salerno**, 2019, pp. 269–287.
- [21] S. Vitale, F.D. Tramparulo, S. Ciarcia, F.O. Amore, E.P. Prinzi, F. Laiena, *The northward tectonic transport in the southern Apennines: examples from the Capri Island and western*

- Sorrento Peninsula (Italy), **Int. J. Earth Sci.** **106**, 2017, pp. 97–113. doi:10.1007/s00531-016-1300-9.
- [22] G. Carannante, R. Graziano, G. Pappone, D. Ruberti, L. Simone, *Depositional system and response to sea level oscillations of the Senonian rudist-bearing carbonate shelves. Examples from central Mediterranean areas*, **Facies**, 1999 pp. 1–24.
- [23] S. Vitale, S. Ciarcia, *Tectono-stratigraphic setting of the Campania region (Southern Italy)*, **J. Maps.** **14**, 2018, pp.9–21. doi:10.1080/17445647.2018.1424655.
- [24] H. Sigurdsson, S. Carey, W. Cornell, T. Pescatore, *The eruption of Vesuvius in AD 79*, **Natl. Geogr. Res.** **1**, 1985, pp. 332–387.
- [25] R. Santacroce, R. Cioni, P. Marianelli, A. Sbrana, R. Sulpizio, G. Zanchetta, D.J. Donahue, J.L. Joron, *Age and whole rock-glass compositions of proximal pyroclastics from the major explosive eruptions of Somma-Vesuvius: A review as a tool for distal tephrostratigraphy*, **J. Volcanol. Geotherm. Res.** **177**, 2008, pp. 1–18. doi:10.1016/j.jvolgeores.2008.06.009.
- [26] C. Scarpati, A. Perrotta, G.F. De Simone, *Impact of explosive volcanic eruptions around Vesuvius: a story of resilience in Roman time*, **Bull. Volcanol.** **78**, 2016, pp. 1–6. doi:10.1007/s00445-016-1017-4.
- [27] G. Di Maio, Positano 79 AD - *The Roman villa and the Vesuvian eruption*, <https://marpositano.it/en/vesuvian-eruption-79ad>, 2019.
- [28] AA. VV., *The leisure villa, MAR Positano*, **Operaedizioni Salerno, Positano**, 2019, p. 280.
- [29] M. de Gennaro, D. Calcaterra, A. Langella, *Le pietre storiche della Campania - dall'oblio alla riscoperta*, **Luciano Editore, Napoli**, 2013, p. 380.
- [30] P. Kastenmeier, G. Di Maio, G. Balassonex, M. Boni, M. Joachimski, N. Mondillo, *The source of stone building materials from the Pompeii archaeological area and its surroundings*, **Period. Mineral.** **79**, 2010, pp. 39–58. doi:10.2451/2010PM0020.
- [31] M. de Gennaro, P. Cappelletti, A. Langella, A. Perrotta, C. Scarpati, *Genesis of zeolites in the Neapolitan Yellow Tuff: Geological, volcanological and mineralogical evidence*, **Contrib. to Mineral. Petrol.** **139**, 2000, pp. 17–35. doi:10.1007/s004100050571.
- [32] L. Fedele, C. Scarpati, M. Lanphere, L. Melluso, V. Morra, A. Perrotta, G. Ricci, *The Breccia Museo formation, Campi Flegrei, southern Italy: Geochronology, chemostratigraphy and relationship with the Campanian Ignimbrite eruption*, **Bull. Volcanol.** **70**, 2008, pp. 1189–1219. doi:10.1007/s00445-008-0197-y.
- [33] L. Pappalardo, L. Civetta, M. D'Antonio, A. Deino, M. Di Vito, G. Orsi, A. Carandente, S. De Vita, R. Isaia, M. Piochi, *Chemical and Sr-isotopical evolution of the Phlegraean magmatic system before the Campanian Ignimbrite and the Neapolitan Yellow Tuff eruptions*, **J. Volcanol. Geotherm. Res.** **91**, 1999, pp. 141–166. doi:10.1016/S0377-0273(99)00033-5.
- [34] S.K. Gebauer, A.K. Schmitt, L. Pappalardo, D.F. Stockli, O.M. Lovera, *Crystallization and eruption ages of Breccia Museo (Campi Flegrei caldera, Italy) plutonic clasts and their relation to the Campanian ignimbrite*, **Contrib. to Mineral. Petrol.** **167**, 2014, pp. 1–18. doi:10.1007/s00410-013-0953-7.
- [35] B. Giaccio, I. Hajdas, R. Isaia, A. Deino, S. Nomade, *High-precision  $^{14}\text{C}$  and  $^{40}\text{Ar}/^{39}\text{Ar}$  dating of the Campanian Ignimbrite (Y-5) reconciles the time-scales of climatic-cultural processes at 40 ka*, **Sci. Rep.** **7**, 2017, doi:10.1038/srep45940.
- [36] A. Langella, D.L. Bish, P. Cappelletti, G. Cerri, A. Colella, R. de Gennaro, S.F. Graziano, A. Perrotta, C. Scarpati, M. de Gennaro, *New insights into the mineralogical facies distribution of Campanian Ignimbrite, a relevant Italian industrial material*, **Appl. Clay Sci.** **72**, 2013, pp. 55–73. doi:10.1016/j.clay.2013.01.008.
- [37] A.L. Deino, G. Orsi, S. de Vita, M. Piochi, *The age of the Neapolitan Yellow Tuff caldera-forming eruption (Campi Flegrei caldera - Italy) assessed by  $^{40}\text{Ar}/^{39}\text{Ar}$  dating method*, **J. Volcanol. Geotherm. Res.** **133**, 2004, pp. 157–170. doi:10.1016/S0377-0273(03)00396-2.
- [38] V. Di Renzo, M.A. Di Vito, I. Arienzo, A. Carandente, L. Civetta, M. D'Antonio, F. Giordano, G. Orsi, S. Tonarini, *Magmatic history of Somma-Vesuvius on the basis of new*

- geochemical and isotopic data from a deep borehole (Camaldoli della Torre)*, **J. Petrol.** **48**, 2007, pp. 753–784. doi:10.1093/petrology/egl081.
- [39] F. Izzo, A. Arizzi, P. Cappelletti, G. Cultrone, A. De Bonis, C. Germinario, S.F. Graziano, C. Grifa, V. Guarino, M. Mercurio, V. Morra, A. Langella, *The art of building in the Roman period (89 B.C. - 79 A.D.): Mortars, plasters and mosaic floors from ancient Stabiae (Naples, Italy)*, **Constr. Build. Mater.** **117**, 2016, pp. 129–143. doi:10.1016/j.conbuildmat.2016.04.101.
- [40] R. Piovesan, E. Curti, C. Grifa, L. Maritan, C. Mazzoli, *Ancient plaster technology: petrographic and microstratigraphic analysis of plaster-based building materials from the Temple of Venus, Pompeii*, in: **Interpret. Silent Artefacts Petrogr. Approaches to Archaeol. Ceram.**, P.S. Quinn, Archaeopress, Oxford, 2009, pp. 65–79.
- [41] Ente Italiano di Normazione, UNI 11305:2009 - *Beni culturali - Malte storiche - Linee guida per la caratterizzazione mineralogico-petrografica, fisica e chimica delle malte*, 2009.
- [42] J. Siivola, R. Schmid, *List of Mineral abbreviations, IUGS Subcomm. Syst. Metamorph. Rocks*, 2007, pp. 1–14.
- [43] M. Bartolini, B. Davide, E. Giani, A. Guglielmi, F. Talarico, *The study of the state of preservation and the technical characteristics of the frescoed surfaces of the Roman age*, in: **Leisure. Villa, MAR Positano, Operaedizioni Salerno**, 2019, pp. 269–278.
- [44] C. Grifa, L. Cavassa, A. De Bonis, C. Germinario, V. Guarino, F. Izzo, I. Kakoulli, A. Langella, M. Mercurio, V. Morra, I. Lloyd, *Beyond Vitruvius: New Insight in the Technology of Egyptian Blue and Green Frits*, **J. Am. Ceram. Soc.** **99**, 2016, pp. 3467–3475. doi:10.1111/jace.14370.
- [45] A.H. Munsell, *Color Soil Charts*, 1994.
- [46] B. Fabbri, S. Gualtieri, S. Shoval, *The presence of calcite in archeological ceramics*, **J. Eur. Ceram. Soc.** **34**, 2014, pp. 1899–1911. doi:10.1016/j.jeurceramsoc.2014.01.007.
- [47] R.A. Kemp, *Soil micromorphology and the quaternary. Quaternary Research Association technical guide no. 2*, London UK Birkbeck College, 1985.
- [48] V. Morra, D. Calcaterra, P. Cappelletti, A. Colella, L. Fedele, R. de Gennaro, A. Langella, M. Mercurio, M. de Gennaro, *Urban geology: Relationships between geological setting and architectural heritage of the Neapolitan area*, **J. Virtual Explor.** **36**, 2010, doi:10.3809/jvirtex.2010.00261.
- [49] B. Scheibner, G. Wörner, L. Civetta, H.-G. Stosch, K. Simon, A. Kronz, *Rare earth element fractionation in magmatic Ca-rich garnets*, **Contrib. Mineral.Petrol.** **154**, 2007, pp.55–74. doi:10.1007/s00410-006-0179-z.
- [50] G. Di Maio, M.A. Iannelli, S. Scala, *Il Paesaggio archeologico e gli effetti dell'eruzione pliniana del 79 d.C. su Salerno e la Costa di Amalfi*, **Kithon Lydios, Stud. Di Stor. e Archeol. Con Giovanna Greco, Naus Ed.**, (2017), pp. 828–851.
- [51] M. Secco, A. Addis, G. Artioli, I. Angelini, *Archaeometric analyses on structural binders*, in: **Leisure Villa, MAR Positano, Operaedizioni Salerno**, 2019, pp. 239–244.
- [52] D. Miriello, D. Barca, A. Bloise, A. Ciarallo, G.M. Crisci, T. De Rose, C. Gattuso, F. Gazineo, M.F. La Russa, *Characterisation of archaeological mortars from Pompeii (Campania, Italy) and identification of construction phases by compositional data analysis*, **J. Archaeol. Sci.** **37**, 2010, pp. 2207–2223. doi:10.1016/j.jas.2010.03.019.
- [53] R. Piovesan, M.C. Dalconi, L. Maritan, C. Mazzoli, *X-ray powder diffraction clustering and quantitative phase analysis on historic mortars*, **Eur. J. Mineral.** **25**, 2013, pp. 165–175. doi:10.1127/0935-1221/2013/0025-2263.

---

Received: December 3, 2019

Accepted: February 27, 2020